# Connected and disconnected contributions to nucleon axial form factors using $N_f$=2 twisted mass fermions at the physical point

**Kyriakos Hadjiyiannakou**

*Computation-based Science and Technology Research Center, The Cyprus Institute*

In collaboration with:

C. Alexandrou, M. Constantinou, K. Jansen, C. Kallidonis, G. Koutsou, A. Vaquero


# Outline

- Introduction
- Lattice evaluation
- Renormalization
- Results for $G_A^{(u-d,\, u+d,\, s)}$
- Results for $G_p^{(u-d,\, u+d,\, s)}$
- Conclusions and future work

# Introduction

- While the nucleon electromagnetic form factors are well known experimentally the axial form factors are known to less accuracy.
- The axial charge $g_A$ is known to high precision from β-decays.

# Introduction

- While the nucleon electromagnetic form factors are well known experimentally the axial form factors are known to less accuracy.
- The axial charge $g_A$ is known to high precision from β-decays.

**Two methods have been extensively used to determine the axial form factor $G_A(Q^2)$ :**

- Elastic scattering of neutrinos and protons $\nu_\mu + n \to \mu^- + p$
- Analysis of charged pion electro-production data

# Introduction

- W … ly the axi…
- T…

**Two m… ) :**

- E…
- A…

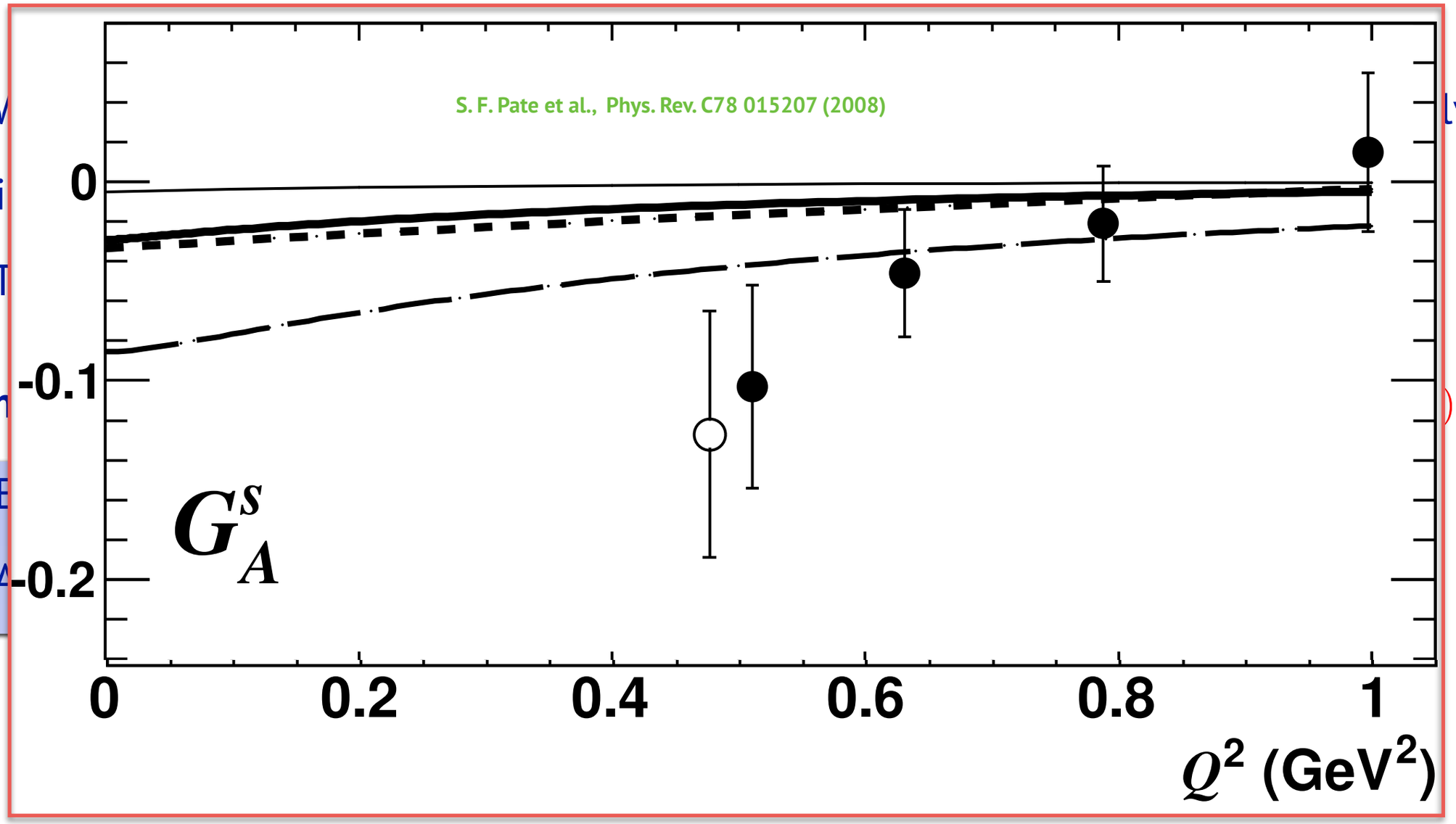

# Introduction

- While the nucleon electromagnetic form factors are well known experimentally the axial form factors are known to less accuracy.
- The axial charge $g_A$ is known to high precision from β-decays.

**Two methods have been extensively used to determine the axial form factor $G_A(Q^2)$ :**

- Elastic scattering of neutrinos and protons $\nu_\mu + n \to \mu^- + p$
- Analysis of charged pion electro-production data

# Introduction

- While the nucleon electromagnetic form factors are well known experimentally the axial form factors are known to less accuracy.
- The axial charge $g_A$ is known to high precision from β-decays.

**Two methods have been extensively used to determine the axial form factor $G_A(Q^2)$ :**

- Elastic scattering of neutrinos and protons $\nu_\mu + n \to \mu^- + p$
- Analysis of charged pion electro-production data

**The induced pseudoscalar form factor $G_p(Q^2)$ is difficult to measure experimentally:**

- The induced pseudoscalar coupling $g_p$ can be measured from muon capture experiments.
- There are few experimental results for $G_p(Q^2)$ from the longitudinal cross section in pion electroproduction data.

# Introduction

- While the nucleon electromagnetic form factors are well known experimentally the axial form factors are known to less accuracy.
- The axial charge $g_A$ is known to high precision from β-decays.

**Two methods have been extensively used to determine the axial form factor $G_A(Q^2)$ :**

- Elastic scattering of neutrinos and protons $\nu_\mu + n \to \mu^- + p$
- Analysis of charged pion electro-production data

**The induced pseudoscalar form factor $G_p(Q^2)$ is difficult to measure experimentally:**

- The induced pseudoscalar coupling $g_p$ can be measured from muon capture experiments.
- There are few experimental results for $G_p(Q^2)$ from the longitudinal cross section in pion electroproduction data.

**With simulations directly at the physical point LQCD can provide predictions for such quantities.**

# Lattice Evaluation

Nucleon axial matrix element decomposition:

$$\langle N(p',s')|A^q_\mu|N(p,s)\rangle \propto \bar{u}_N(p',s')\left(\gamma_\mu G^q_A(Q^2) - i\frac{Q_\mu}{2m_N}G^q_p(Q^2)\right)\gamma_5 u_N(p,s) \qquad A^q_\mu = \bar{q}\gamma_\mu\gamma_5 q$$

At zero momentum transfer: $G^q_A(Q^2=0) \to g^q_A$ $\qquad g^q_A = \int_0^1 dx(\Delta q(x) + \Delta\bar{q}(x))$

- $g^q_A$ is a very important quantity which measures the intrinsic quark spin contribution to the nucleon and the chiral symmetry breaking.

# Lattice Evaluation

Nucleon axial matrix element decomposition:

$$\langle N(p',s')|A^q_\mu|N(p,s)\rangle \propto \bar{u}_N(p',s')\left(\gamma_\mu G^q_A(Q^2) - i\frac{Q_\mu}{2m_N}G^q_p(Q^2)\right)\gamma_5 u_N(p,s) \qquad A^q_\mu = \bar{q}\gamma_\mu\gamma_5 q$$

At zero momentum transfer: $G^q_A(Q^2=0) \to g^q_A$ $\qquad g^q_A = \int_0^1 dx(\Delta q(x) + \Delta\bar{q}(x))$

- $g^q_A$ is a very important quantity which measures the intrinsic quark spin contribution to the nucleon and the chiral symmetry breaking.

Three- and two-point functions: $G(t_s, \mathrm{t_{ins}}, t_0) = \langle J(t_s)A_\mu(\mathrm{t_{ins}})\bar{J}(t_0)\rangle$, $C(t_s,t_0) = \langle J(t_s)\bar{J}(t_0)\rangle$

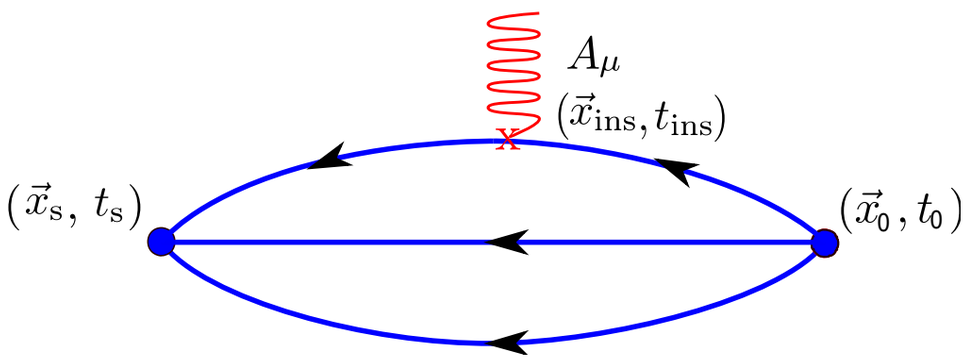

# Lattice Evaluation

Nucleon axial matrix element decomposition:

$$\langle N(p',s')|A^q_\mu|N(p,s)\rangle \propto \bar{u}_N(p',s')\left(\gamma_\mu G^q_A(Q^2) - i\frac{Q_\mu}{2m_N}G^q_p(Q^2)\right)\gamma_5 u_N(p,s) \qquad A^q_\mu = \bar{q}\gamma_\mu\gamma_5 q$$

At zero momentum transfer: $G^q_A(Q^2=0) \to g^q_A$ $\qquad g^q_A = \int_0^1 dx(\Delta q(x) + \Delta\bar{q}(x))$

- $g^q_A$ is a very important quantity which measures the intrinsic quark spin contribution to the nucleon and the chiral symmetry breaking.

Three- and two-point functions: $G(t_s, \mathrm{t_{ins}}, t_0) = \langle J(t_s)A_\mu(\mathrm{t_{ins}})\bar{J}(t_0)\rangle$, $C(t_s,t_0) = \langle J(t_s)\bar{J}(t_0)\rangle$

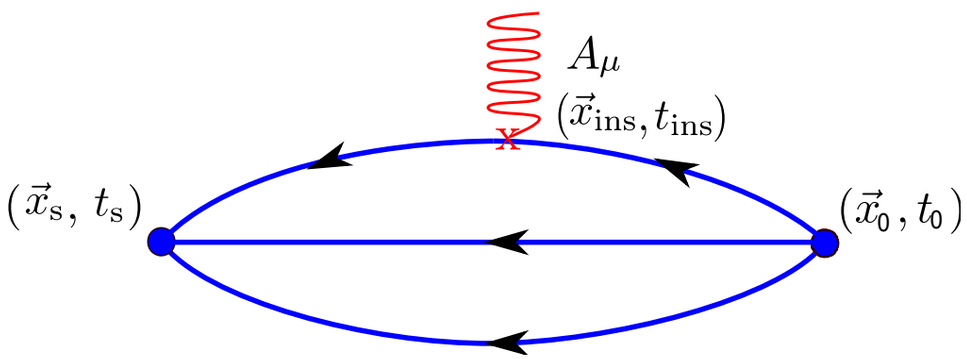


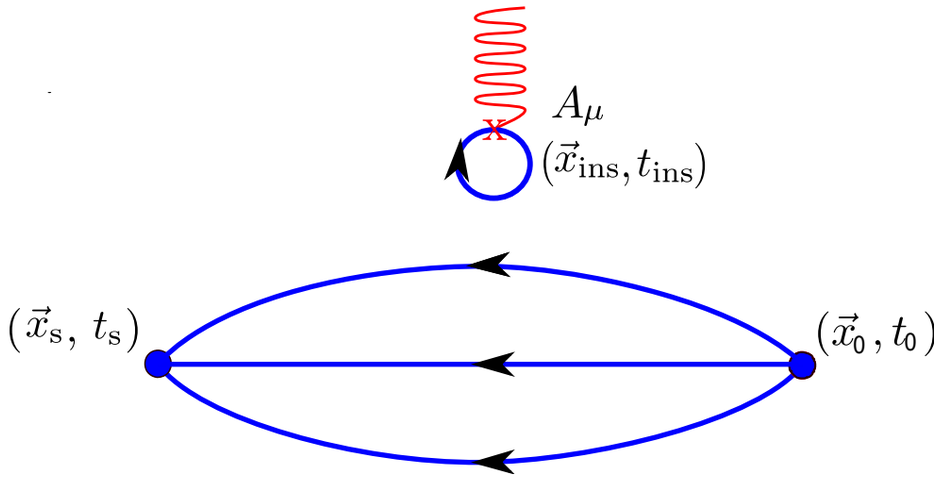

# Lattice Evaluation

Nucleon axial matrix element decomposition:

$$\langle N(p',s')|A^q_\mu|N(p,s)\rangle \propto \bar{u}_N(p',s')\left(\gamma_\mu G^q_A(Q^2) - i\frac{Q_\mu}{2m_N}G^q_p(Q^2)\right)\gamma_5 u_N(p,s) \qquad A^q_\mu = \bar{q}\gamma_\mu\gamma_5 q$$

At zero momentum transfer: $G^q_A(Q^2=0) \to g^q_A$ $\qquad g^q_A = \int_0^1 dx(\Delta q(x) + \Delta\bar{q}(x))$

- $g^q_A$ is a very important quantity which measures the intrinsic quark spin contribution to the nucleon and the chiral symmetry breaking.

Three- and two-point functions: $G(t_s, \mathrm{t_{ins}}, t_0) = \langle J(t_s)A_\mu(\mathrm{t_{ins}})\bar{J}(t_0)\rangle$, $C(t_s,t_0) = \langle J(t_s)\bar{J}(t_0)\rangle$

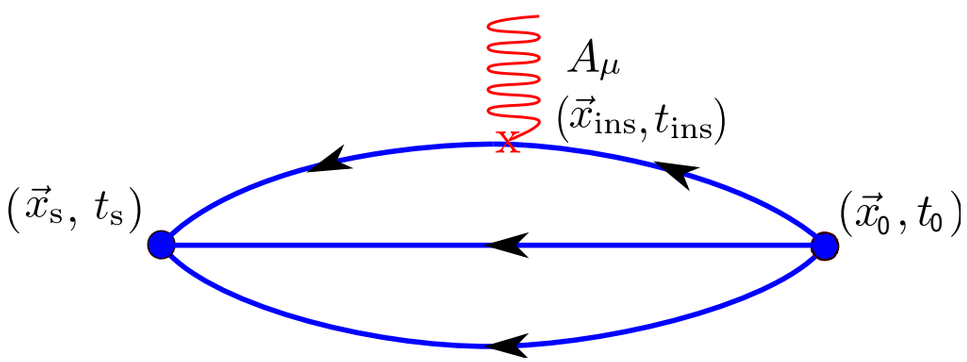


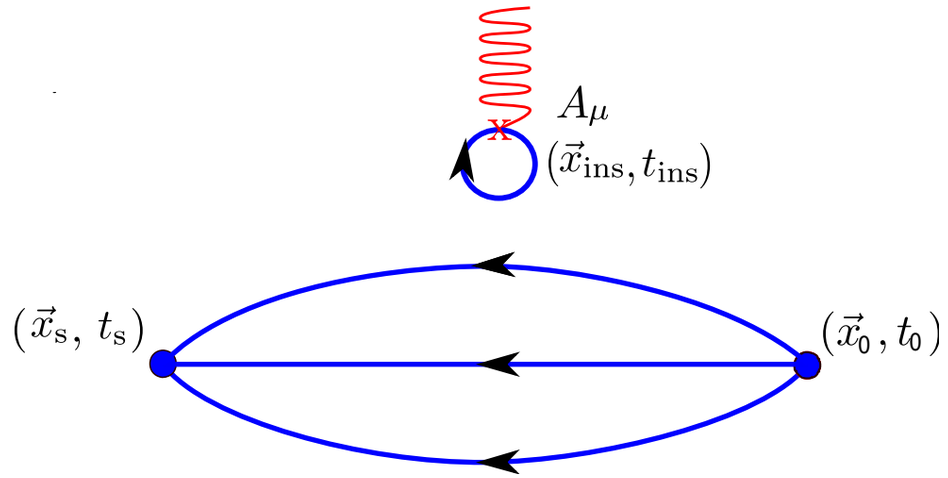


- In the isovector case disconnected quark loop contributions cancel out.
- In the isoscalar both connected and disconnected contribute.
- Strange and charm contributions are purely disconnected.

# Lattice Evaluation

Disconnected quark loops are **prohibitively expensive** → all-to-all propagator

$$L^{(f)}(t_{\rm ins},\vec{q}) = \sum_{\vec{x}_{\rm ins}} {\rm Tr}\left[M_f^{-1}(x_{\rm ins};x_{\rm ins})\mathcal{G}\right] e^{i\vec{q}\cdot\vec{x}_{\rm ins}}$$

# Lattice Evaluation

Disconnected quark loops are **prohibitively expensive** → all-to-all propagator

$$L^{(f)}(t_{\rm ins},\vec{q}) = \sum_{\vec{x}_{\rm ins}} {\rm Tr}\left[M_f^{-1}(x_{\rm ins};x_{\rm ins})\mathcal{G}\right] e^{i\vec{q}\cdot\vec{x}_{\rm ins}}$$

- Estimation of quark loops using **stochastic techniques.**
- **One-end trick** for twisted mass fermions, for axial → **generalized** version:

C. McNeile, C. Michael, Phys. Rev. D73 074506 (2006), 0603007

$$\begin{aligned} L^{u+d}(t_{\rm ins};\vec{q}) &= \sum_{\vec{x}_{\rm ins}} {\rm Tr}\left[(M_u^{-1}(x_{\rm ins};x_{\rm ins}) + M_d^{-1}(x_{\rm ins};x_{\rm ins}))\mathcal{G}\right] e^{i\vec{q}\cdot\vec{x}_{\rm ins}} \\ &= 2\sum_{\vec{x}_{\rm ins}}\sum_{y,y'} {\rm Tr}\left[M_d^{-1^\dagger}(y';x_{\rm ins})\gamma_5\mathcal{G}\gamma_5 D_{WC}(x_{\rm ins};y)M_d^{-1}(y;y')\right] e^{i\vec{q}\cdot\vec{x}_{\rm ins}} \end{aligned}$$

→ Allows **better signal-to-noise** behavior.

# Lattice Evaluation

Disconnected quark loops are **prohibitively expensive** → all-to-all propagator

$$L^{(f)}(t_{\rm ins},\vec{q}) = \sum_{\vec{x}_{\rm ins}} {\rm Tr}\left[M_f^{-1}(x_{\rm ins};x_{\rm ins})\mathcal{G}\right] e^{i\vec{q}\cdot\vec{x}_{\rm ins}}$$

- Estimation of quark loops using **stochastic techniques.**
- **One-end trick** for twisted mass fermions, for axial → **generalized** version:

C. McNeile, C. Michael, Phys. Rev. D73 074506 (2006), 0603007

$$\begin{aligned} L^{u+d}(t_{\rm ins};\vec{q}) &= \sum_{\vec{x}_{\rm ins}} {\rm Tr}\left[(M_u^{-1}(x_{\rm ins};x_{\rm ins}) + M_d^{-1}(x_{\rm ins};x_{\rm ins}))\mathcal{G}\right] e^{i\vec{q}\cdot\vec{x}_{\rm ins}} \\ &= 2\sum_{\vec{x}_{\rm ins}}\sum_{y,y'} {\rm Tr}\left[M_d^{-1^\dagger}(y';x_{\rm ins})\gamma_5\mathcal{G}\gamma_5 D_{WC}(x_{\rm ins};y)M_d^{-1}(y;y')\right] e^{i\vec{q}\cdot\vec{x}_{\rm ins}} \end{aligned}$$

→ Allows **better signal-to-noise** behavior.

Study of **excited states** → **three methods**:

- **Plateau Method:** Assumes just one state dominance, fit to a constant
- **Summation Method:**

$$R_\mu^{\rm sum}(\Gamma_\nu,\vec{q},t_s) \equiv \sum_{t_{\rm ins}=a}^{t_s-a} R_\mu(\Gamma_\nu,\vec{q},t_s,t_{\rm ins}) = C + t_s\mathcal{M} + \mathcal{O}(e^{-\Delta t_s}) + \cdots$$

- **Two-State Method:**
  - Takes into account the first excited state.
  - Simultaneous fit to three- and two-point functions.

# Renormalization

To compare with experimental and phenomenological results, lattice results should be **renormalized**.

- We perform a **non-perturbative** calculation.
- **Lattice artifacts** were computed **perturbatively** up to 1-loop.
- **Rome-Southampton**[*] method, **Landau gauge-fixed** configurations → vertex functions.

G. Martinelli et. al., Nucl. Phys., B445 (1995), 9411010

# Renormalization

To compare with experimental and phenomenological results, lattice results should be **renormalized**.

- We perform a **non-perturbative** calculation.
- **Lattice artifacts** were computed **perturbatively** up to 1-loop.
- **Rome-Southampton**[*] method, **Landau gauge-fixed** configurations ⟶ vertex functions.

G. Martinelli et. al., Nucl. Phys., B445 (1995), 9411010

$$G^{ns}_{\mathcal{G}}(p) = \frac{a^{12}}{V}\sum_{x,y,z} e^{-ip(x-y)}\langle u(x)\bar{u}(z)\mathcal{G}d(z)\bar{d}(y)\rangle, \quad G^{s}_{\mathcal{G}}(p) = \frac{a^{12}}{V}\sum_{x,y,z} e^{-ip(x-y)}\langle u(x)\bar{u}(z)\mathcal{G}u(z)\bar{u}(y)\rangle$$

The singlet vertex function involves **disconnected quark loops** and is more difficult to compute.

# Renormalization

To compare with experimental and phenomenological results, lattice results should be **renormalized**.

- We perform a **non-perturbative** calculation.
- **Lattice artifacts** were computed **perturbatively** up to 1-loop.
- **Rome-Southampton**[*] method, **Landau gauge-fixed** configurations ⟶ vertex functions.

G. Martinelli et. al., Nucl. Phys., B445 (1995), 9411010

$$G^{ns}_{\mathcal{G}}(p) = \frac{a^{12}}{V}\sum_{x,y,z} e^{-ip(x-y)}\langle u(x)\bar{u}(z)\mathcal{G}d(z)\bar{d}(y)\rangle, \quad G^{s}_{\mathcal{G}}(p) = \frac{a^{12}}{V}\sum_{x,y,z} e^{-ip(x-y)}\langle u(x)\bar{u}(z)\mathcal{G}u(z)\bar{u}(y)\rangle$$

The singlet vertex function involves **disconnected quark loops** and is more difficult to compute.

- Amputation of the vertex functions using the inverse propagators is performed.
- We impose the $\text{RI}_{\text{MOM}}$ condition.

$$\Lambda_{\mathcal{G}}(p) = (S(p))^{-1} G_{\mathcal{G}}(p) (S(p))^{-1}, \quad Z_q^{-1}\mathbf{Z}_{\mathcal{G}}\text{Tr}\left[\Lambda_{\mathcal{G}}(p)\Lambda^{\text{tree}}_{\mathcal{G}}\right] = \text{Tr}\left[\Lambda^{\text{tree}}_{\mathcal{G}}\,\Lambda^{\text{tree}}_{\mathcal{G}}\right]$$

# Renormalization

C. Alexandrou et al., arXiv: 1705.03399

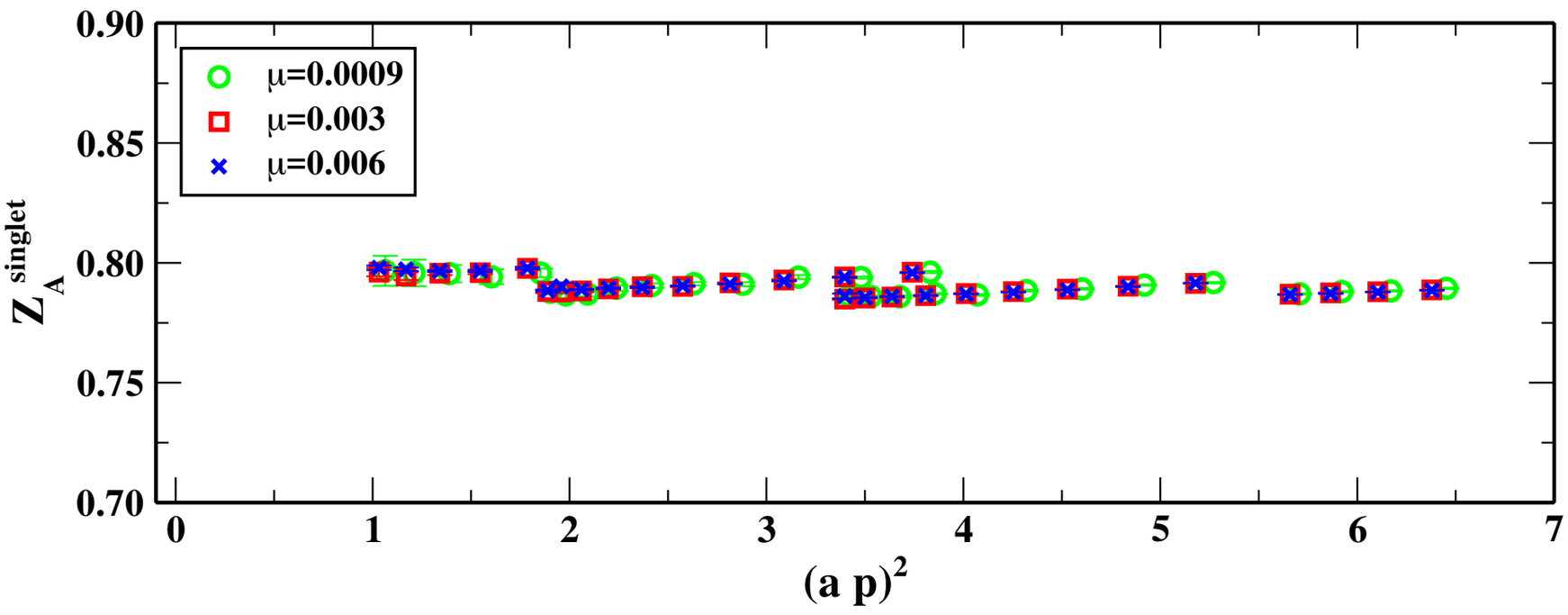


- Vertex functions for three pion masses, extrapolation to the chiral limit
- Several values of $(ap)^2$, extrapolation in the limit $(ap)^2 \to 0$

# Renormalization

C. Alexandrou et al., arXiv: 1705.03399

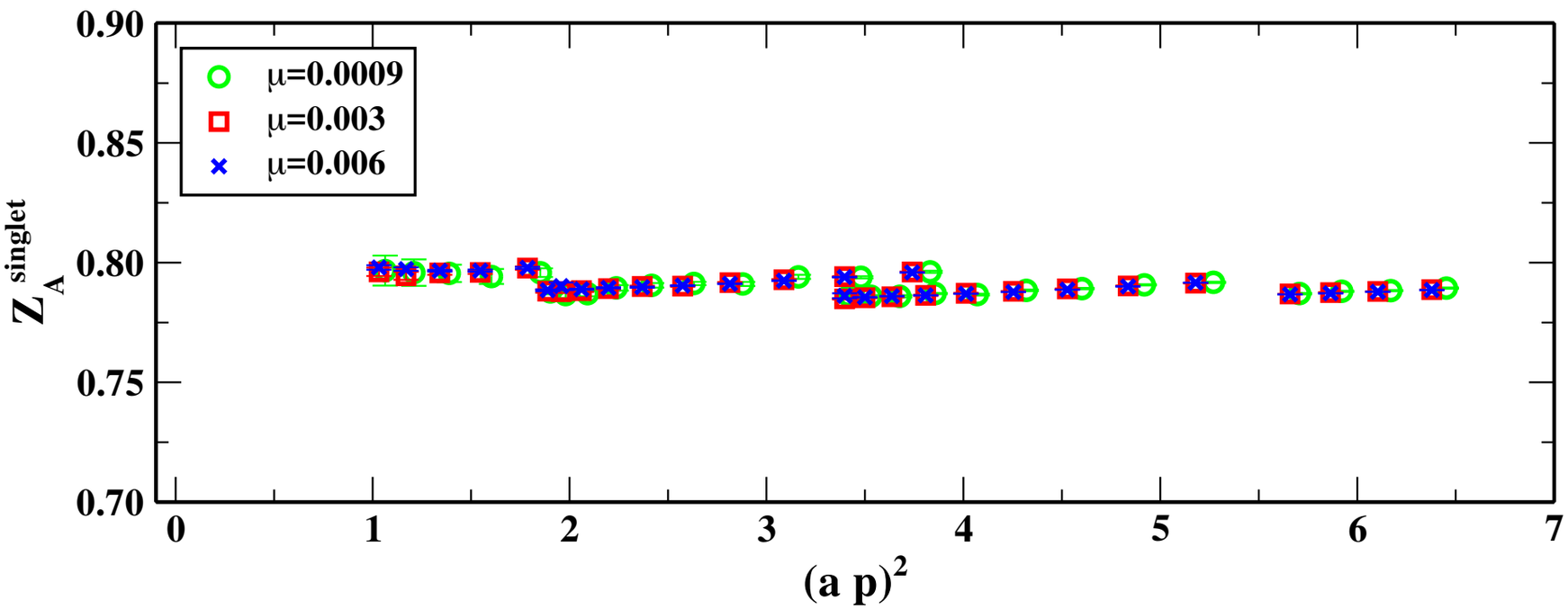


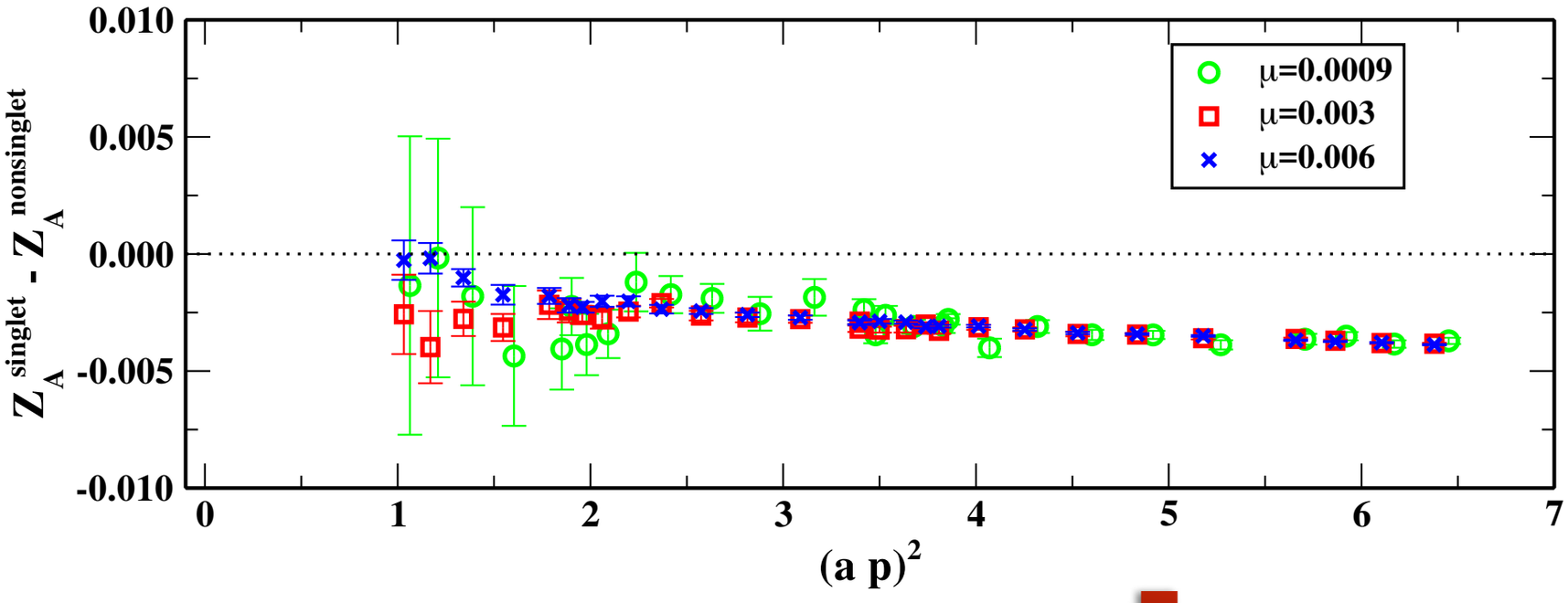


- Vertex functions for three pion masses, extrapolation to the chiral limit
- Several values of $(ap)^2$, extrapolation in the limit $(ap)^2 \to 0$

**The difference between singlet and non-singlet renormalization has been found to be small.**

# Simulation Details

- Simulations by the **ETM** collaboration (ETMC) A. Abdel-Rehim et al. Phys. Rev. D95 094525 (2017), 1507.05068
- One ensemble of $\mathbf{N_f = 2}$ **twisted mass** clover improved fermions
- Lattice size: $\mathbf{48^3 x 96}$
- Lattice spacing: **a = 0.0938(3)(2) fm** determined from the nucleon mass
- $\mathbf{m_\pi = 130\ MeV}$
- **Osterwalder-Seiler** fermions for the **strange** and **charm** quarks

# Simulation Details

- Simulations by the **ETM** collaboration (ETMC) A. Abdel-Rehim et al. Phys. Rev. D95 094525 (2017), 1507.05068
- One ensemble of $\mathbf{N_f = 2}$ **twisted mass** clover improved fermions
- Lattice size: $\mathbf{48^3 x 96}$
- Lattice spacing: **a = 0.0938(3)(2) fm** determined from the nucleon mass
- $\mathbf{m_\pi = 130\ MeV}$
- **Osterwalder-Seiler** fermions for the **strange** and **charm** quarks

**Maximally twisted fermions:** R. Frezzotti, G. C. Rossi, JHEP 0408 (2004) 007, 0306014

- Automatic $\mathcal{O}(a)$ improvement
- No operator improvement needed, simplified renormalization for hadron structure

# Simulation Details

- Simulations by the **ETM** collaboration (ETMC) A. Abdel-Rehim et al. Phys. Rev. D95 094525 (2017), 1507.05068
- One ensemble of $\mathbf{N_f = 2}$ **twisted mass** clover improved fermions
- Lattice size: $\mathbf{48^3 x 96}$
- Lattice spacing: **a = 0.0938(3)(2) fm** determined from the nucleon mass
- $\mathbf{m_\pi = 130\ MeV}$
- **Osterwalder-Seiler** fermions for the **strange** and **charm** quarks

**Maximally twisted fermions:** R. Frezzotti, G. C. Rossi, JHEP 0408 (2004) 007, 0306014

- Automatic $\mathcal{O}(a)$ improvement
- No operator improvement needed, simplified renormalization for hadron structure

**Statistics:**

| Connected | | | Disconnected | | | | |
|---|---|---|---|---|---|---|---|
| $t_s/a$ | $N_{\text{conf}}$ | $N_{\text{src}}$ | Flavor | $N_{\text{conf}}$ | $N_r^{\text{HP}}$ | $N_r^{\text{LP}}$ | $N_{\text{src}}$ |
| 10 | 579 | 16 | light | 2120 | 2250 | - | 100 |
| 12 | 579 | 16 | strange | 2057 | 63 | 1024 | 100 |
| 14 | 579 | 16 | charm | 2034 | 5 | 1250 | 100 |

# Simulation Details

- Simulations by the **ETM** collaboration (ETMC) A. Abdel-Rehim et al. Phys. Rev. D95 094525 (2017), 1507.05068
- One ensemble of $\mathbf{N_f = 2}$ **twisted mass** clover improved fermions
- Lattice size: $\mathbf{48^3 x 96}$
- Lattice spacing: **a = 0.0938(3)(2) fm** determined from the nucleon mass
- $\mathbf{m_\pi = 130\ MeV}$
- **Osterwalder-Seiler** fermions for the **strange** and **charm** quarks

**Maximally twisted fermions:** R. Frezzotti, G. C. Rossi, JHEP 0408 (2004) 007, 0306014

- Automatic $\mathcal{O}(a)$ improvement
- No operator improvement needed, simplified renormalization for hadron structure

**Statistics:**

| Connected | | | Disconnected | | | | |
|---|---|---|---|---|---|---|---|
| $t_s/a$ | $N_{\text{conf}}$ | $N_{\text{src}}$ | Flavor | $N_{\text{conf}}$ | $N_r^{\text{HP}}$ | $N_r^{\text{LP}}$ | $N_{\text{src}}$ |
| 10 | 579 | 16 | light | 2120 | 2250 | - | 100 |
| 12 | 579 | 16 | strange | 2057 | 63 | 1024 | 100 |
| 14 | 579 | 16 | charm | 2034 | 5 | 1250 | 100 |

Deflated-CG: 600 eigenvectors
20x speedup

# Simulation Details

- Simulations by the **ETM** collaboration (ETMC) A. Abdel-Rehim et al. Phys. Rev. D95 094525 (2017), 1507.05068
- One ensemble of $\mathbf{N_f = 2}$ **twisted mass** clover improved fermions
- Lattice size: $\mathbf{48^3 x 96}$
- Lattice spacing: **a = 0.0938(3)(2) fm** determined from the nucleon mass
- $\mathbf{m_\pi = 130\ MeV}$
- **Osterwalder-Seiler** fermions for the **strange** and **charm** quarks

**Maximally twisted fermions:** R. Frezzotti, G. C. Rossi, JHEP 0408 (2004) 007, 0306014

- Automatic $\mathcal{O}(a)$ improvement
- No operator improvement needed, simplified renormalization for hadron structure

**Statistics:**

| Connected | | | Disconnected | | | | |
|---|---|---|---|---|---|---|---|
| $t_s/a$ | $N_{\rm conf}$ | $N_{\rm src}$ | Flavor | $N_{\rm conf}$ | $N_r^{\rm HP}$ | $N_r^{\rm LP}$ | $N_{\rm src}$ |
| 10 | 579 | 16 | light | 2120 | 2250 | - | 100 |
| 12 | 579 | 16 | strange | 2057 | 63 | 1024 | 100 |
| 14 | 579 | 16 | charm | 2034 | 5 | 1250 | 100 |

Deflated-CG: 600 eigenvectors
20x speedup

Truncated Solver Method (TSM)

G. S. Bali et al. Comp. Phys. Comm 181 1570 (2010), 0910.3970

# Simulation Details

- Simulations by the **ETM** collaboration (ETMC) A. Abdel-Rehim et al. Phys. Rev. D95 094525 (2017), 1507.05068
- One ens
- Lattice s
- Lattice s
- $m_\pi$ = 13(
- Osterwal

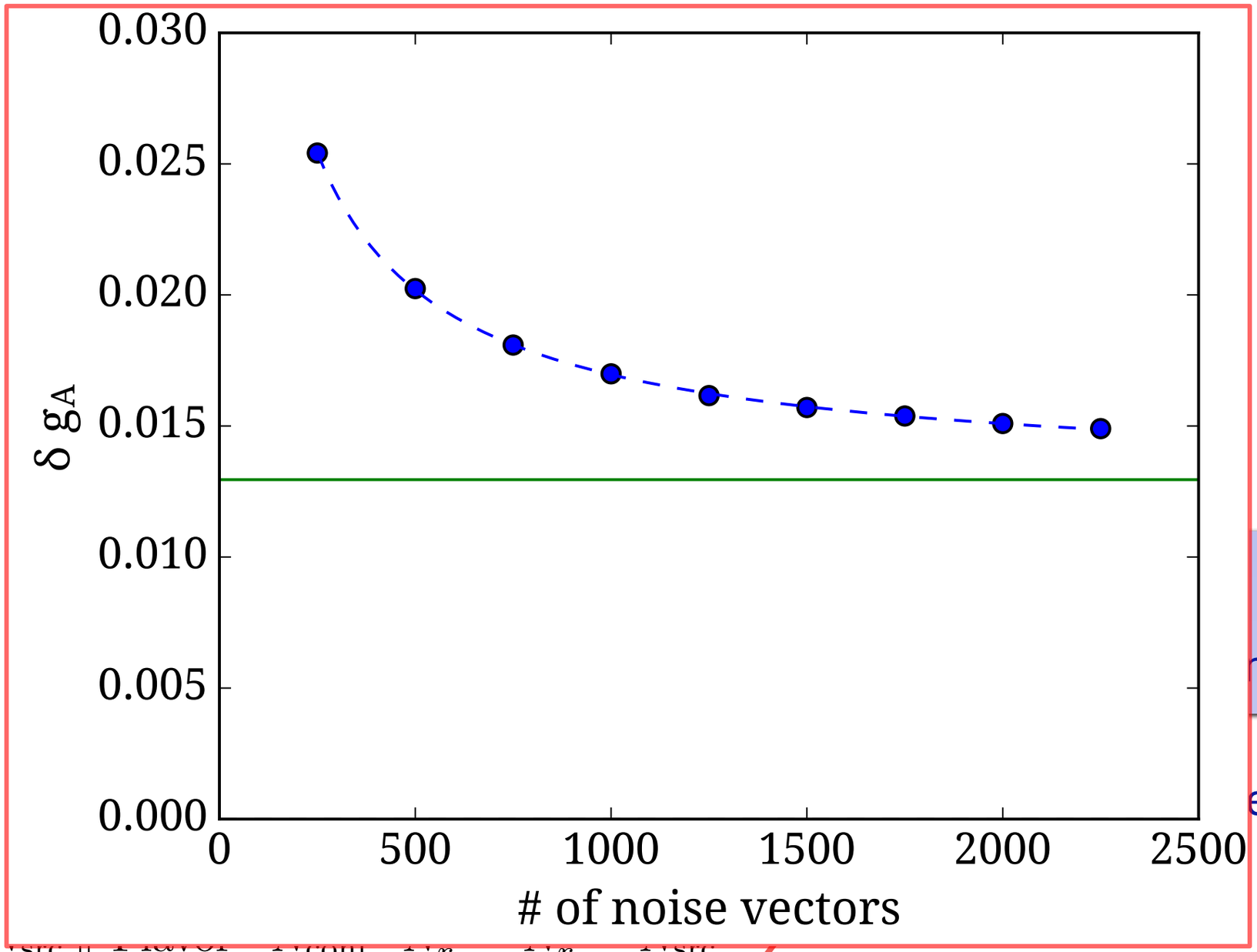


Maximally tw

- Automa
- No oper

n structure

eigenvectors

**Statistics:**

Connectec

| $t_s/a$ | $N_{\rm conf}$ | $N_{\rm src}$ | Flavor | $N_{\rm eig}$ | $N_f$ | $N_f$ | $N_{\rm src}$ |
|---|---|---|---|---|---|---|---|
| 10 | 579 | 16 | light | 2120 | 2250 | - | 100 |
| 12 | 579 | 16 | strange | 2057 | 63 | 1024 | 100 |
| 14 | 579 | 16 | charm | 2034 | 5 | 1250 | 100 |

Truncated Solver Method (TSM)

G. S. Bali et al. Comp. Phys. Comm 181 1570 (2010), 0910.3970

# Results for the nucleon axial charge

C. Alexandrou et al., arXiv: 1705.03399

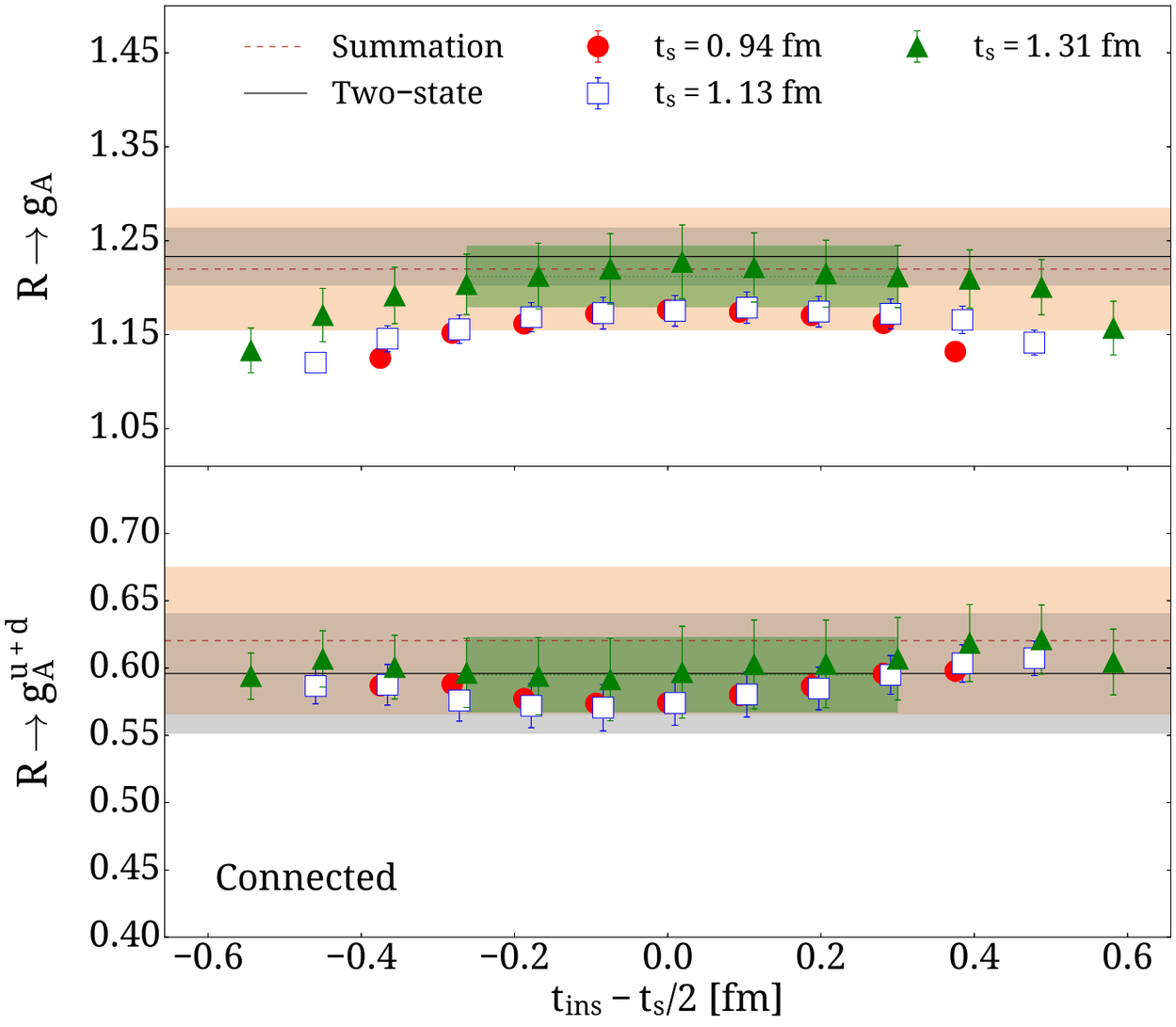


- From the plateau method we find:

$g_A = 1.212(33)(22), \;\; g_A^{u+d}(\text{Conn.}) = 0.595(28)(1)$

# Results for the nucleon axial charge

C. Alexandrou et al., arXiv: 1705.03399

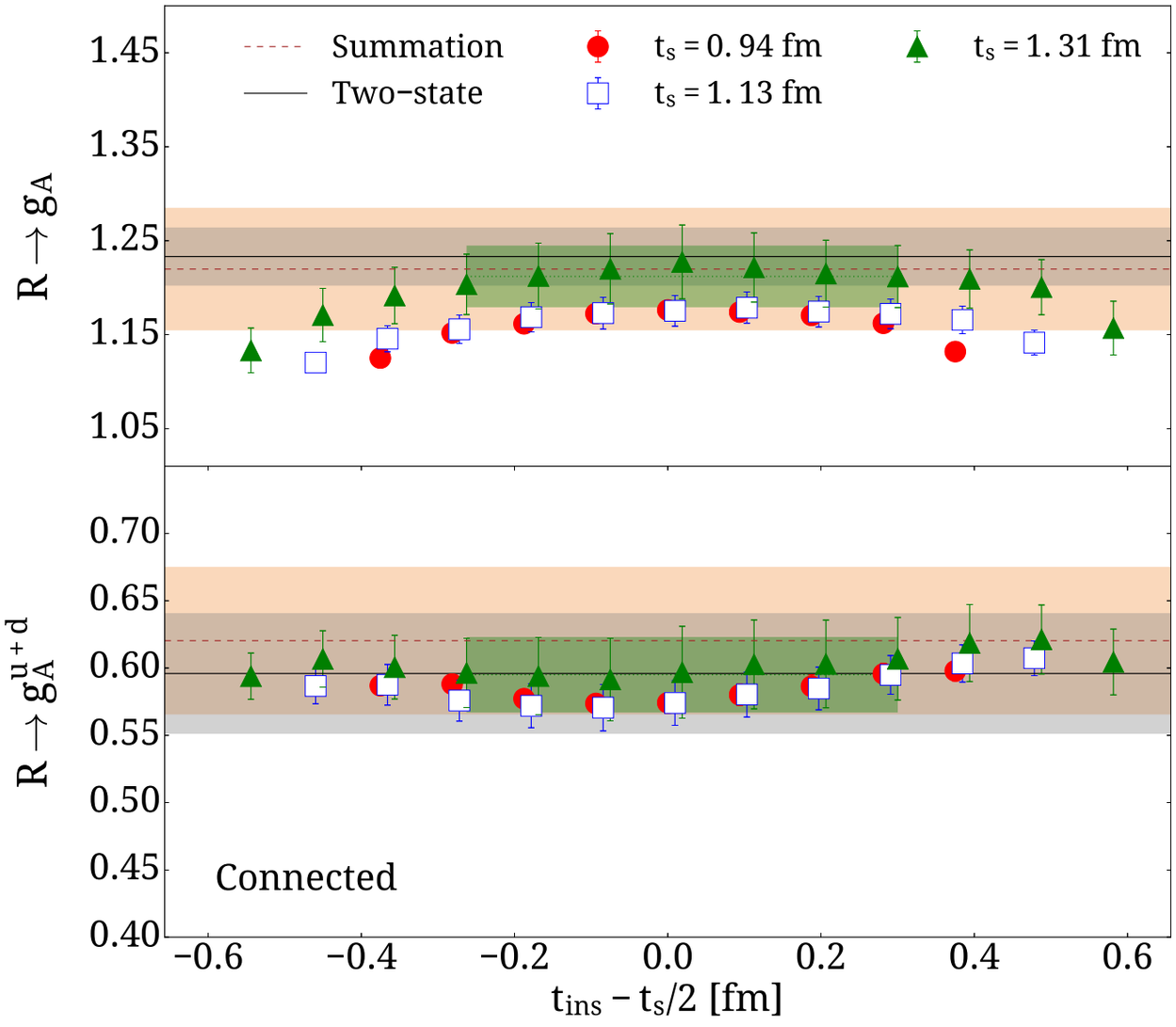


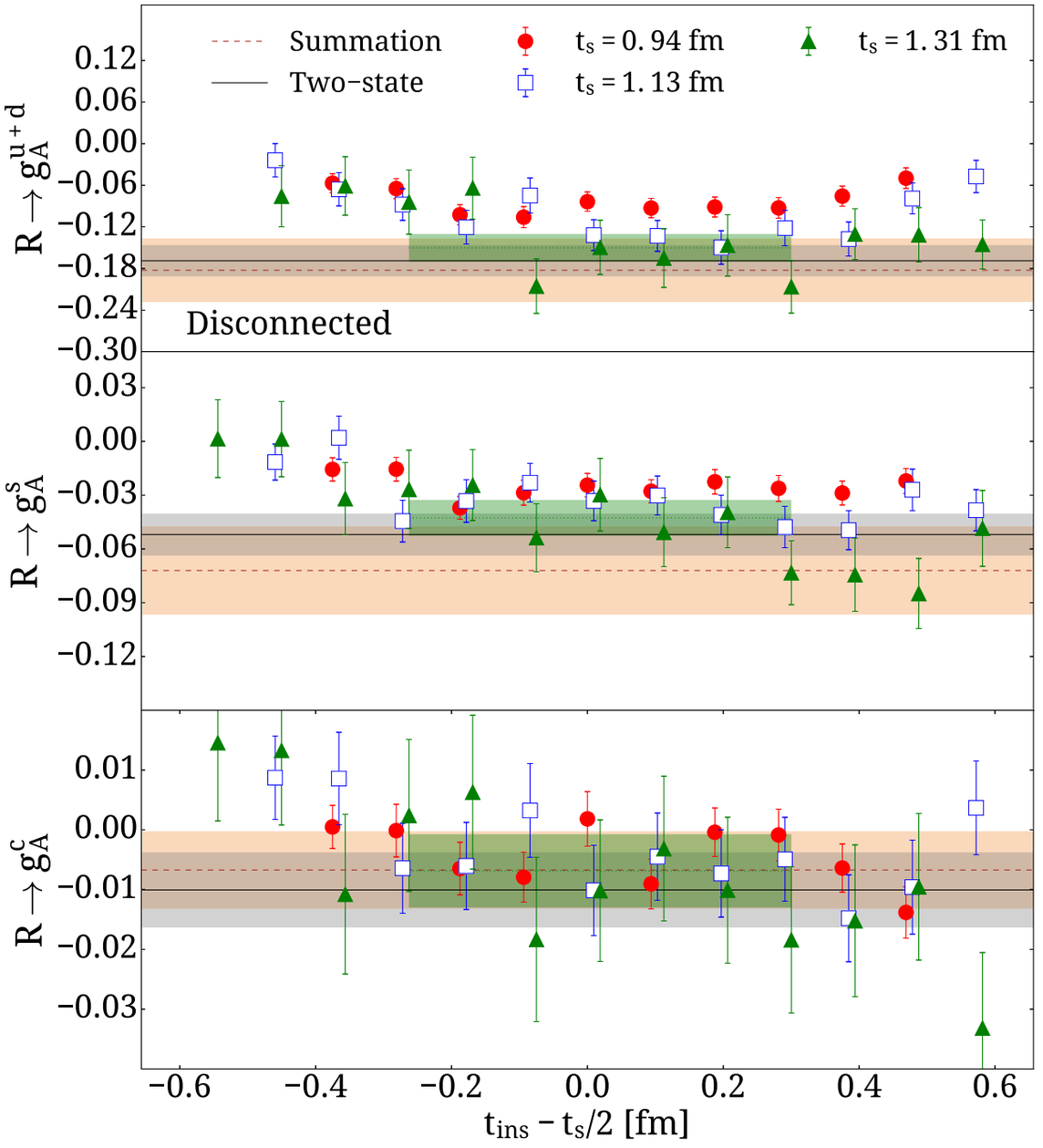


- From the plateau method we find:

$g_A = 1.212(33)(22), \quad g_A^{u+d}(\text{Conn.}) = 0.595(28)(1)$

- Disconnected contributions are negative and non-zero.
- $g_A^{u+d}(\text{Disc.}) = -0.150(20)(19), \quad g_A^{s} = -0.0427(100)(93)$
- Charm tends to be negative but it is noisy.

# Results for $G_A$ and $G_p$ isovector case

C. Alexandrou et al., arXiv: 1705.03399

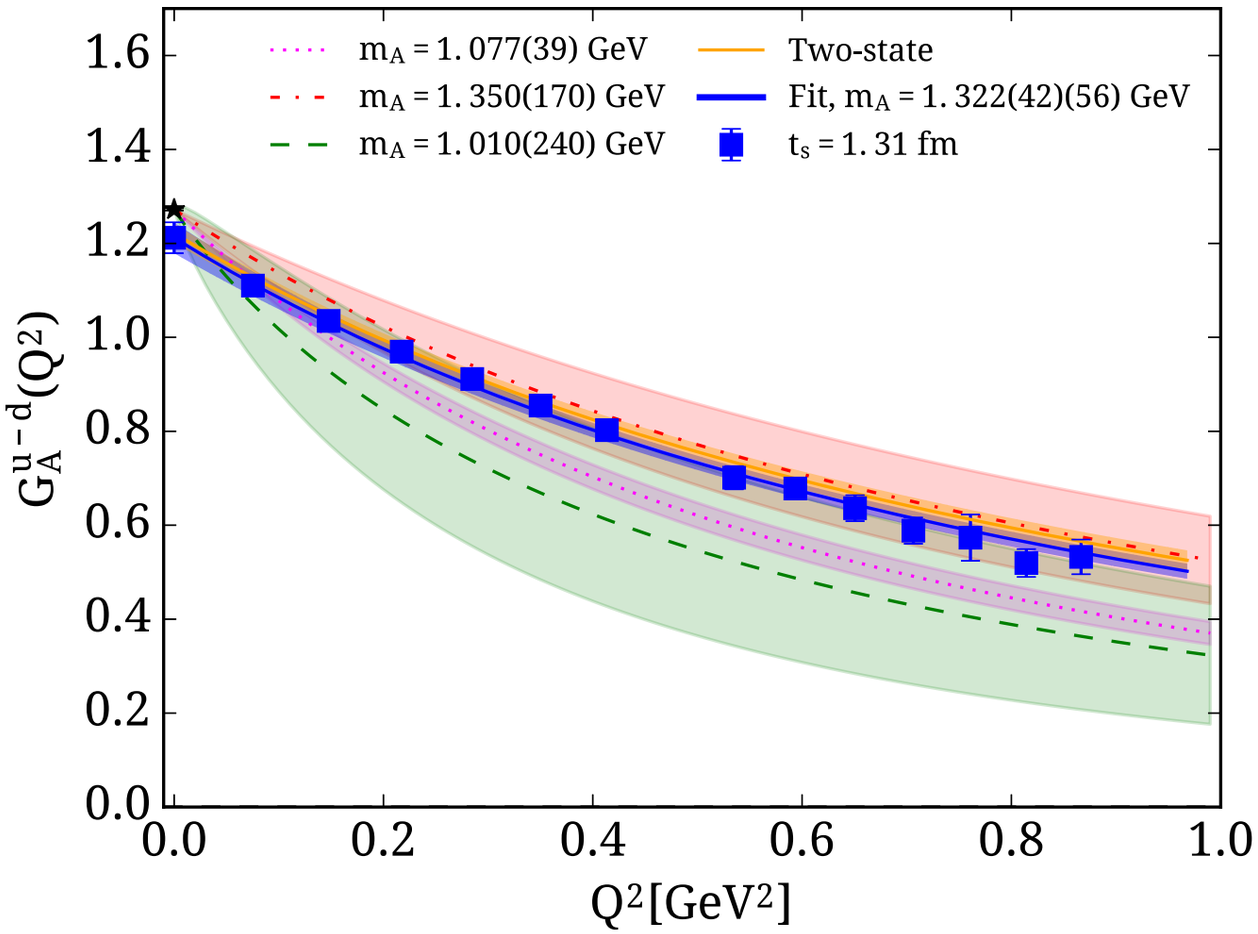


- Fitting using dipole form: $G_A(Q^2) = \frac{g_A}{\left(1 + \frac{Q^2}{m_A^2}\right)^2}$
- Our results are higher than the experimental results from pion electroproduction,

  A. Liesenfeld et al. Phys. Lett. B468 (1999)
- but in agreement with recent results from charged-current muon-neutrino scattering events (MiniBooNE experiment).

  A. A. Aguilar-Arevalo et al. Phys. Rev. D81 092005 (2010)

# Results for $G_A$ and $G_p$ isovector case

C. Alexandrou et al., arXiv: 1705.03399

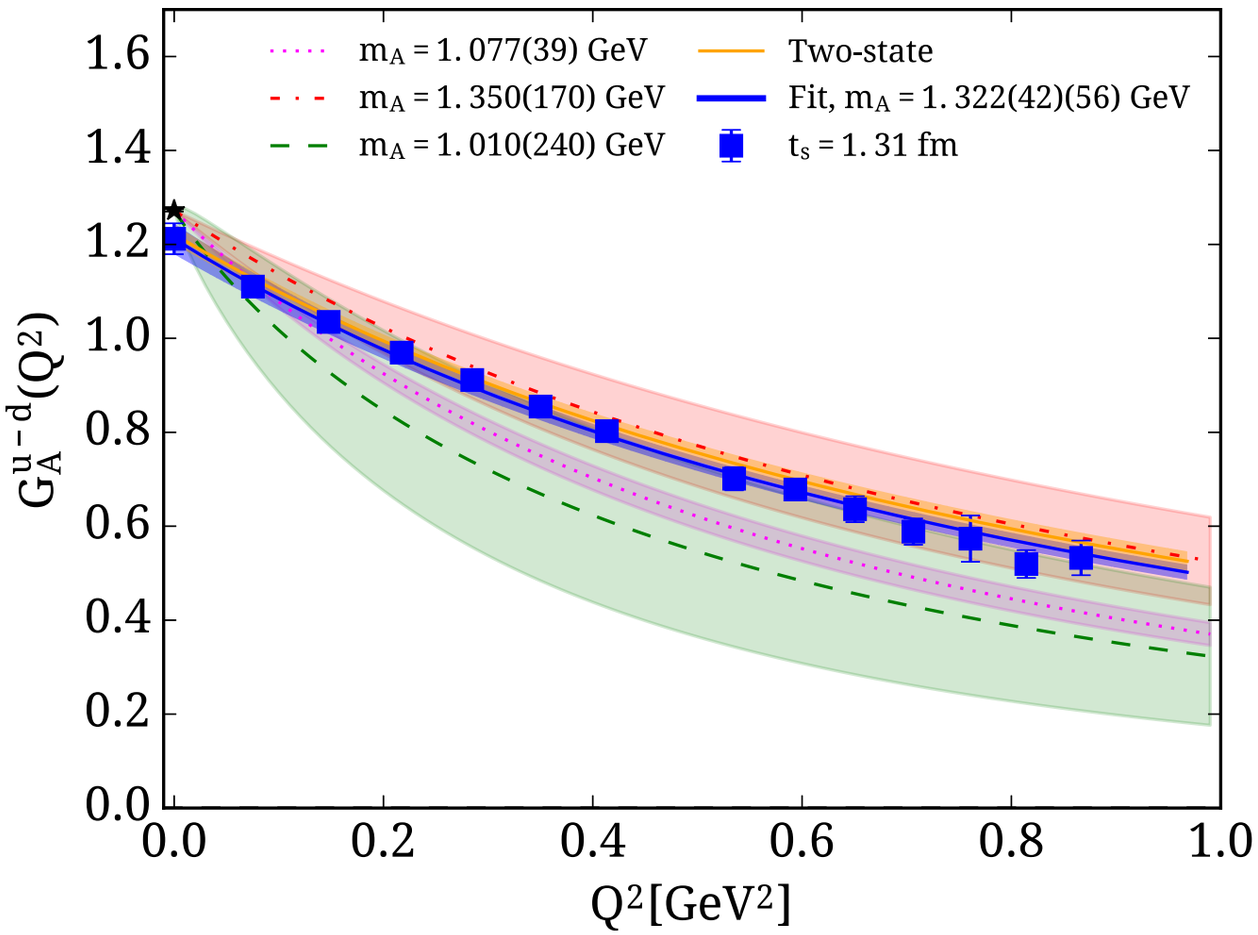


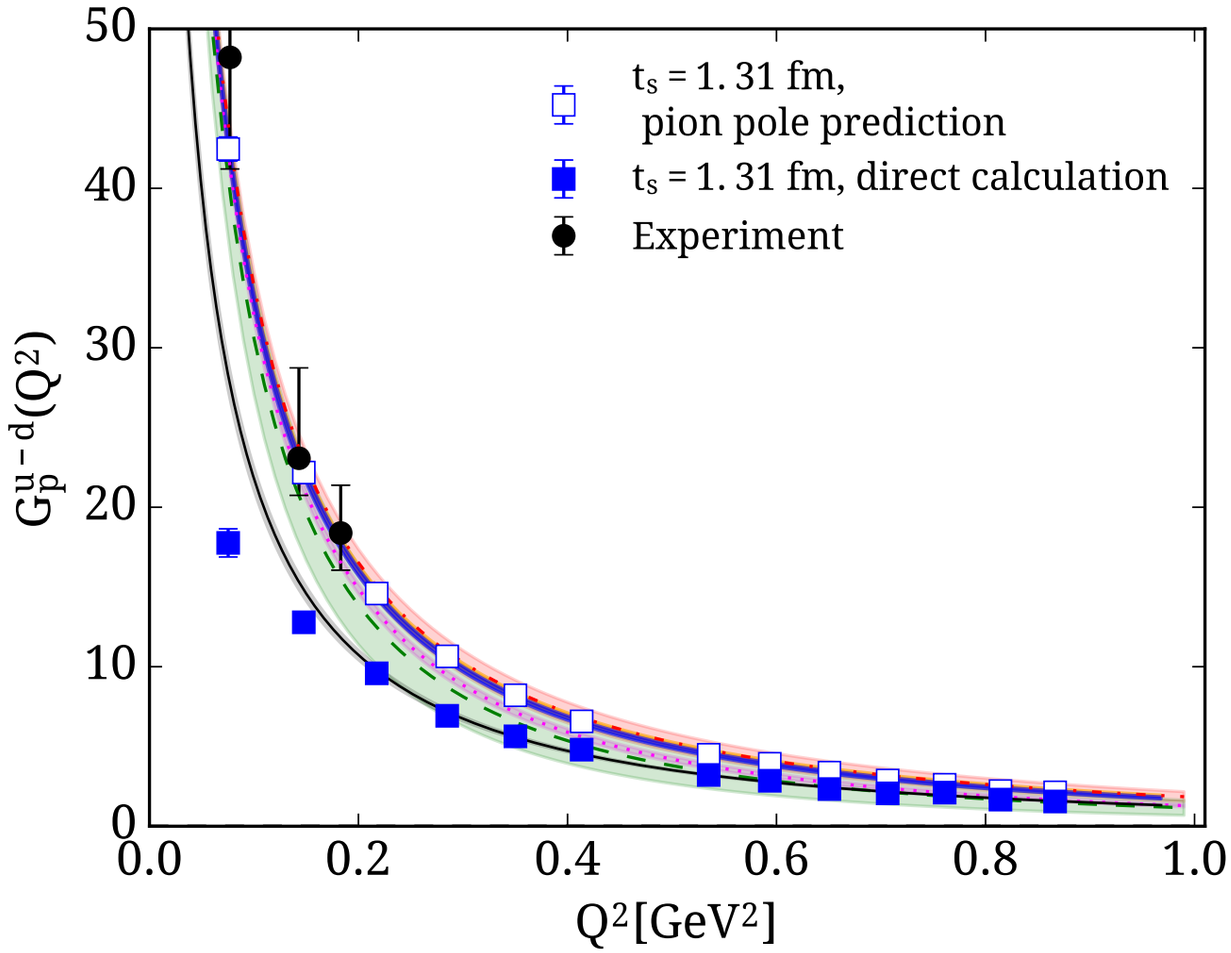


- Fitting using dipole form: $G_A(Q^2) = \frac{g_A}{\left(1+\frac{Q^2}{m_A^2}\right)^2}$
- Our results are higher than the experimental results from pion electroproduction,
  A. Liesenfeld et al. Phys. Lett. B468 (1999)
- but in agreement with recent results from charged-current muon-neutrino scattering events (MiniBooNE experiment).
  A. A. Aguilar-Arevalo et al. Phys. Rev. D81 092005 (2010)

- Fitting using pion pole: $G_p(Q^2) = G_A(Q^2)\frac{4m_N^2}{(Q^2+m_\pi^2)}$
- Few experimental results S. Choi et al. Phys. Rev. Lett. 71 3927 (1993)
- Direct lattice results for $G_p$ rise slowly compared to experimental.
- Lattice results using pion pole prediction are in agreement with the experimental.

# Disconnected contributions to $G_A$ and $G_p$

- For the disconnected, one can produce more intermediate $Q^2$ points without additional cost.
- Dipole and pion pole forms are model dependent.
- One can use the z-expansion (model independent). R. J. Hill, G. Paz, Phys. Rev. D84 073006 (2011)

$$G(Q^2) = \sum_k a_k z(Q^2)^k, \quad z(Q^2) = \frac{\sqrt{t_{cut} + Q^2} - \sqrt{t_{cut}}}{\sqrt{t_{cut} + Q^2} + \sqrt{t_{cut}}}$$

# Disconnected contributions to $G_A$ and $G_p$

- For the disconnected, one can produce more intermediate $Q^2$ points without additional cost.
- Dipole and pion pole forms are model dependent.
- One can use the z-expansion (model independent). R. J. Hill, G. Paz, Phys. Rev. D84 073006 (2011)

$$G(Q^2) = \sum_k a_k z(Q^2)^k, \quad z(Q^2) = \frac{\sqrt{t_{cut} + Q^2} - \sqrt{t_{cut}}}{\sqrt{t_{cut} + Q^2} + \sqrt{t_{cut}}}$$

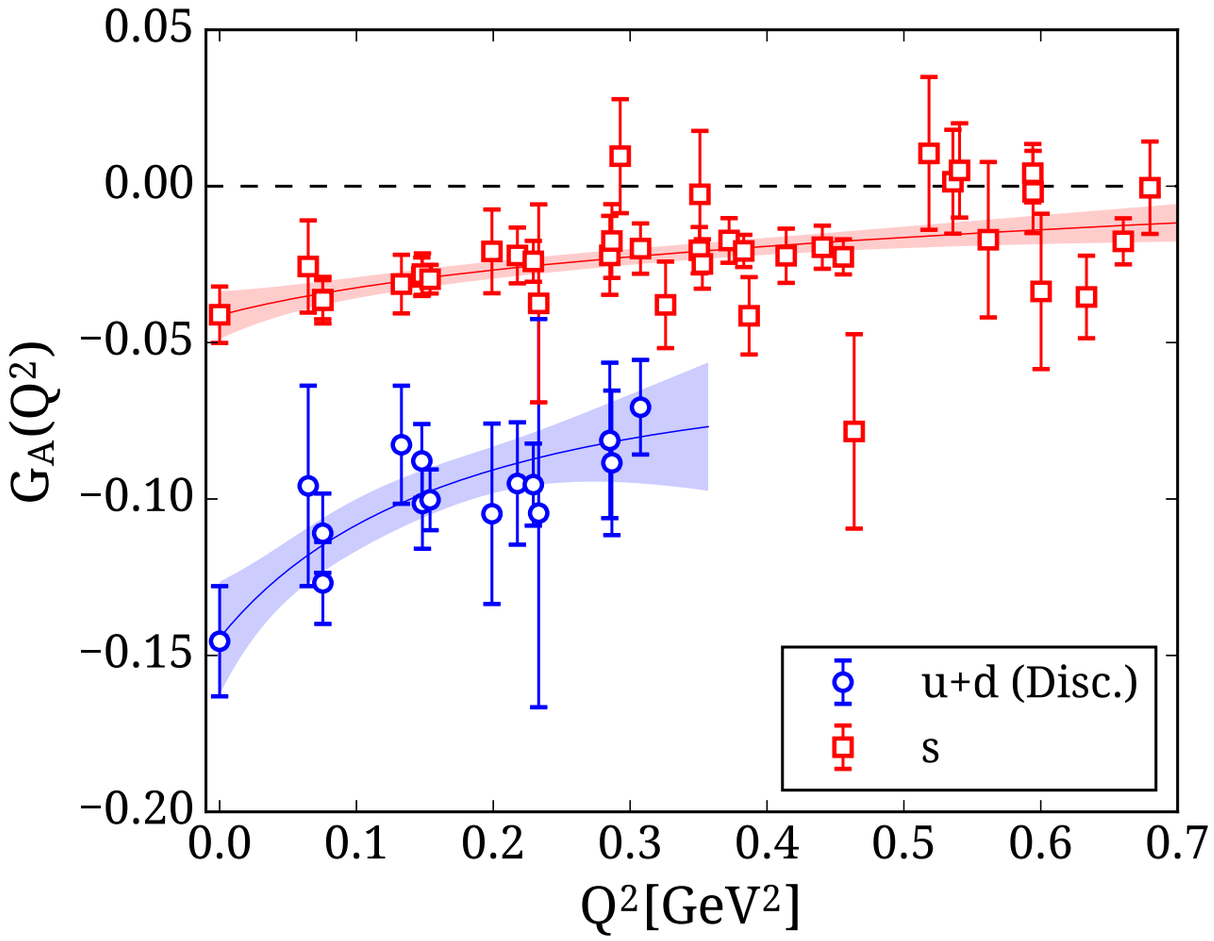

# Disconnected contributions to $G_A$ and $G_p$

- For the disconnected, one can produce more intermediate $Q^2$ points without additional cost.
- Dipole and pion pole forms are model dependent.
- One can use the z-expansion (model independent). R. J. Hill, G. Paz, Phys. Rev. D84 073006 (2011)

$$G(Q^2) = \sum_k a_k z(Q^2)^k, \quad z(Q^2) = \frac{\sqrt{t_{cut} + Q^2} - \sqrt{t_{cut}}}{\sqrt{t_{cut} + Q^2} + \sqrt{t_{cut}}}$$

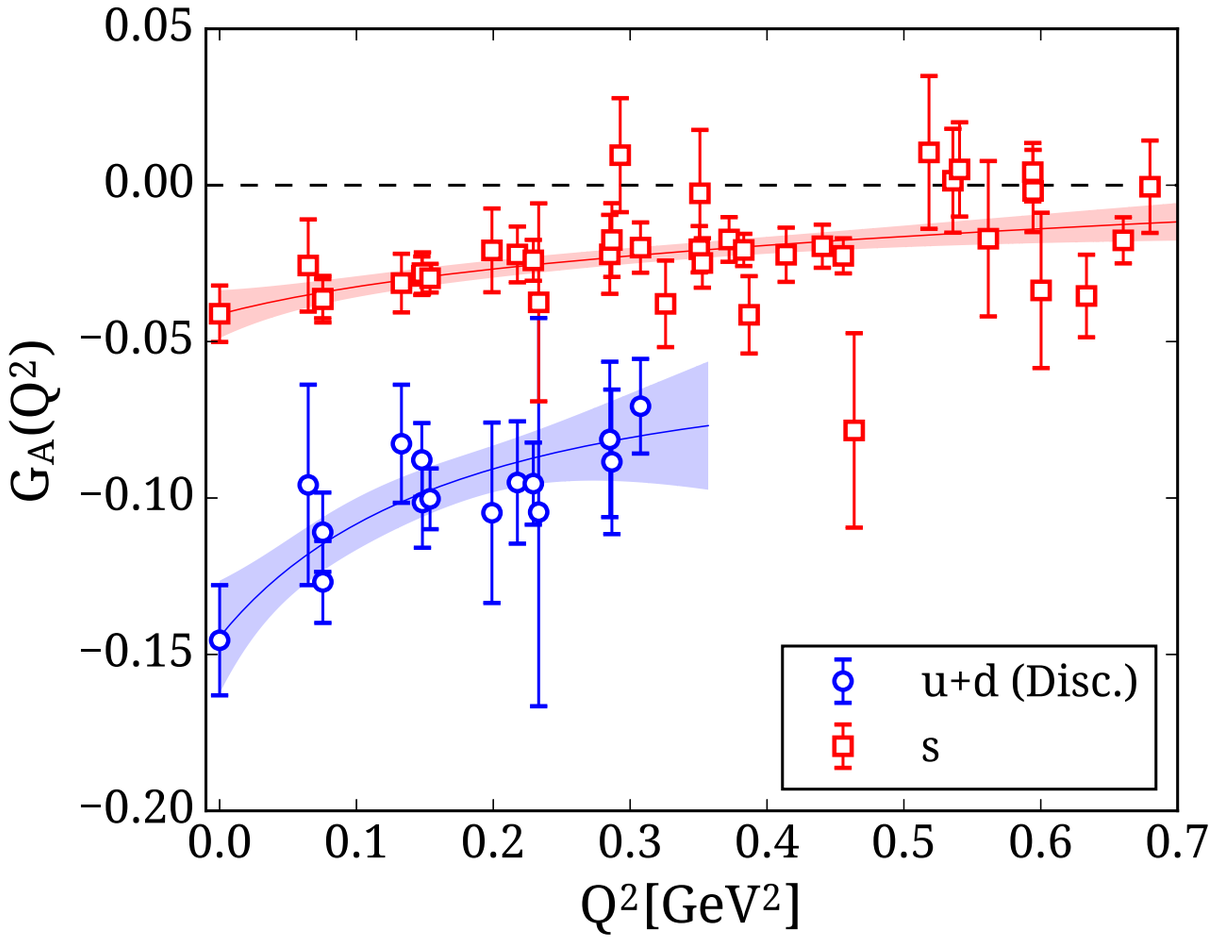


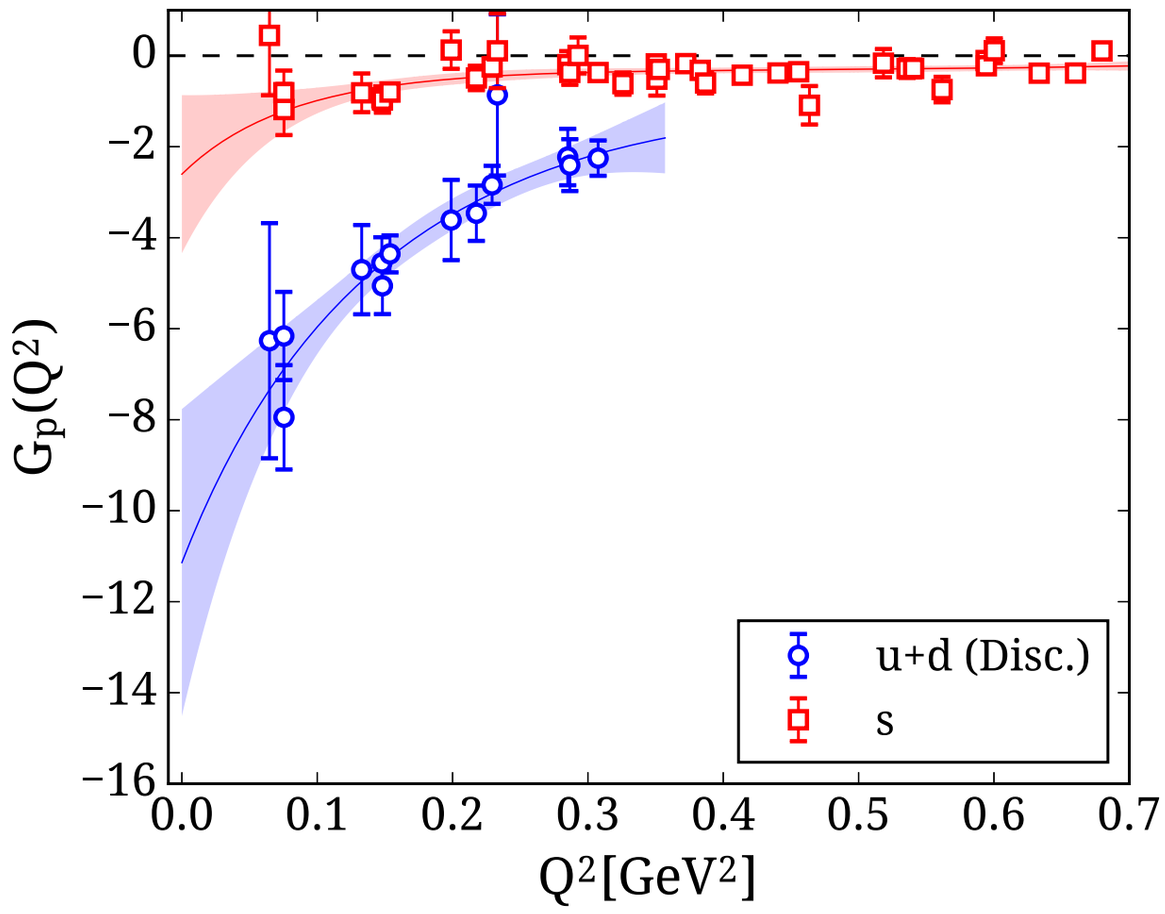


Light and strange disconnected contributions to nucleon axial form factors have been computed accurately on a physical pion mass.

The light disconnected contribution to the induced pseudoscalar form factor is large and negative.

# Total contributions to $G_A$ and $G_p$

C. Alexandrou et al., arXiv: 1705.03399

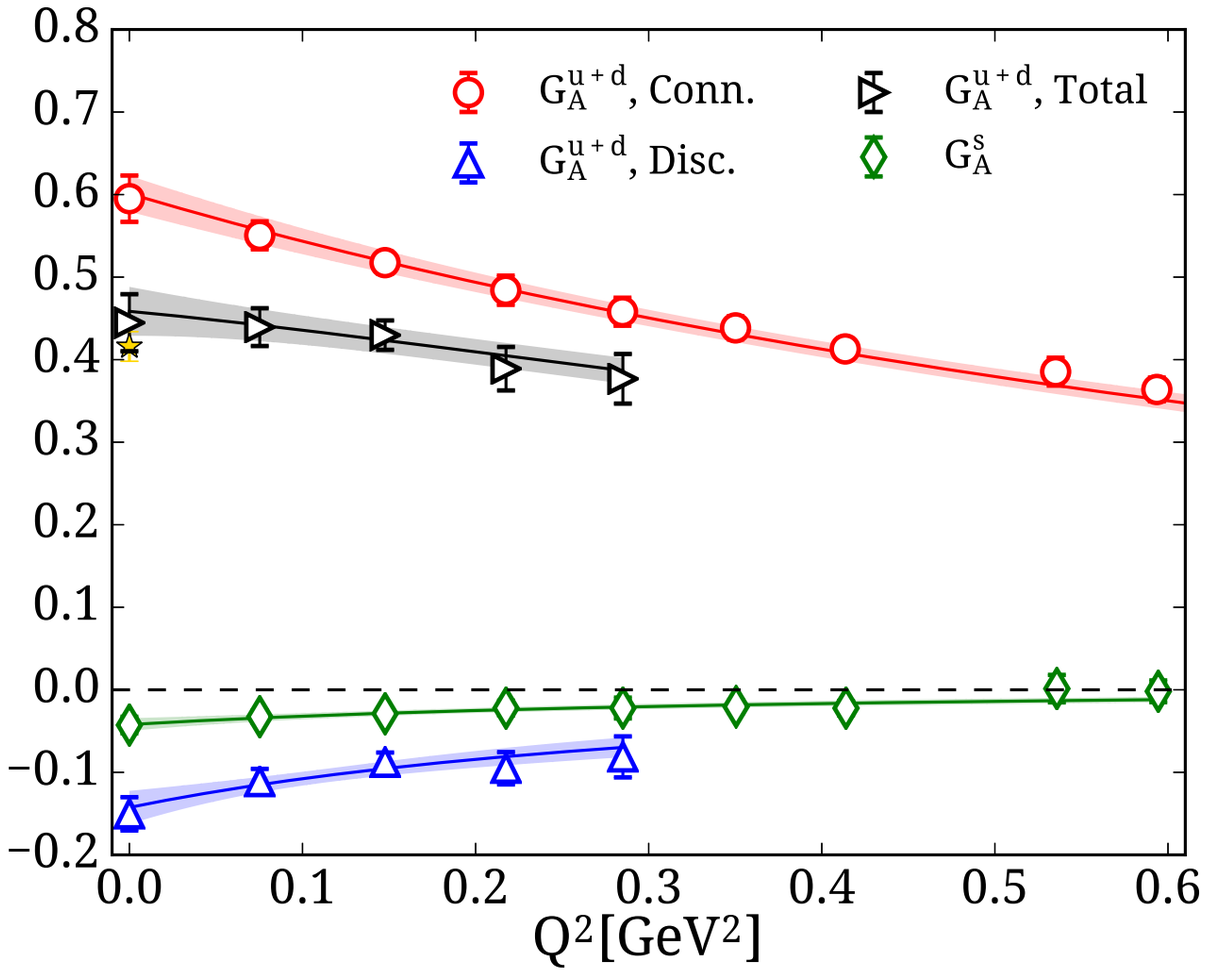


- Disconnected contributions are important in order to bring agreement with $g_A^{u+d}$ experimental.
- Adding connected and disconnected makes the isoscalar axial form factor flatter.
- The strange contribution is about two times smaller than one light quark contribution.

# Total contributions to $G_A$ and $G_p$

C. Alexandrou et al., arXiv: 1705.03399

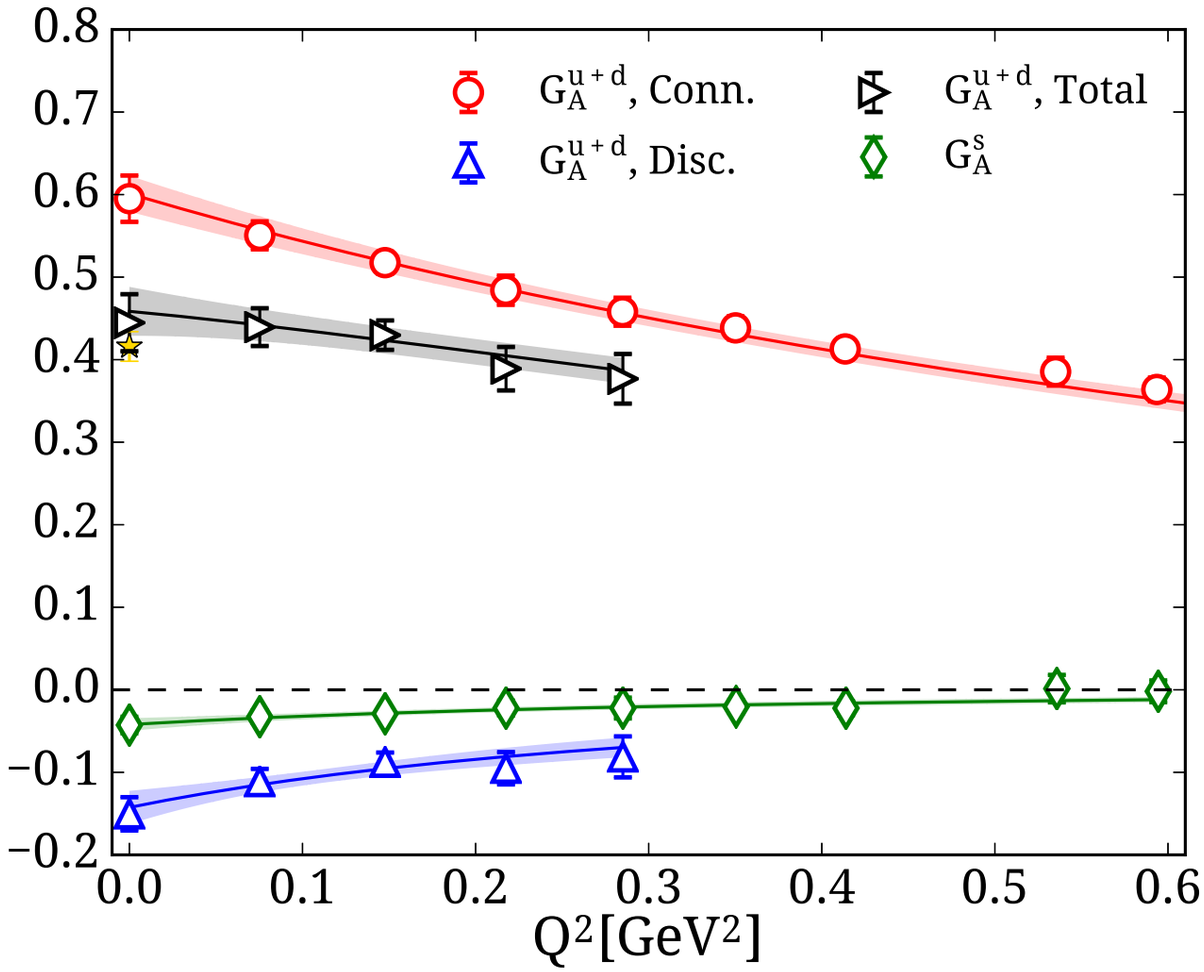


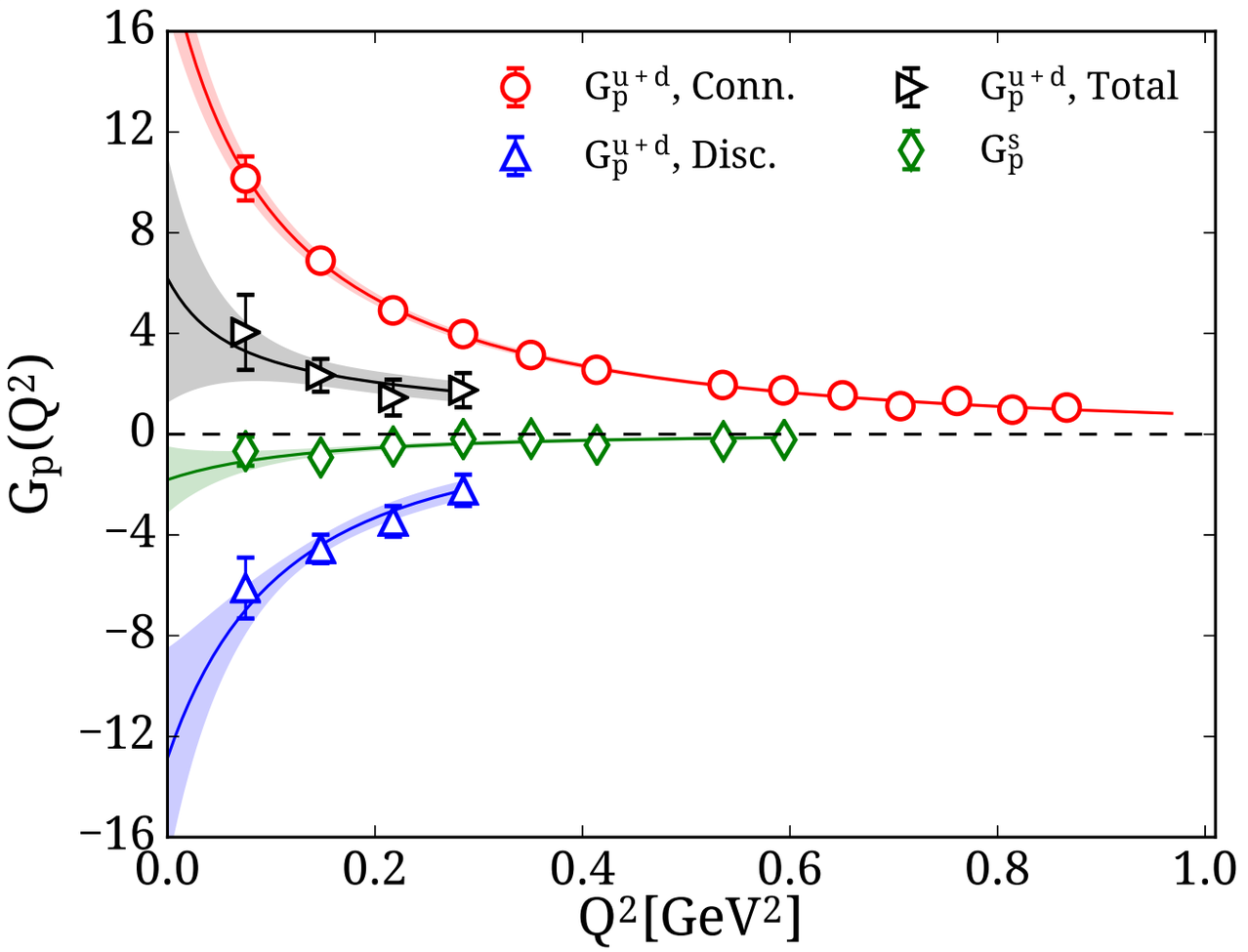


- Disconnected contributions are important in order to bring agreement with $g_A^{u+d}$ experimental.
- Adding connected and disconnected makes the isoscalar axial form factor flatter.
- The strange contribution is about two times smaller than one light quark contribution.

- Results for $G_p^{u+d}$ connected are steep.
- Results for $G_p^{u+d}$ disconnected are also steep coming with a difference sign compared to the connected.
- The total behavior shows a weak $Q^2$-dependence.

# Comparison of $G_A$ and $G_p$ strange with other study

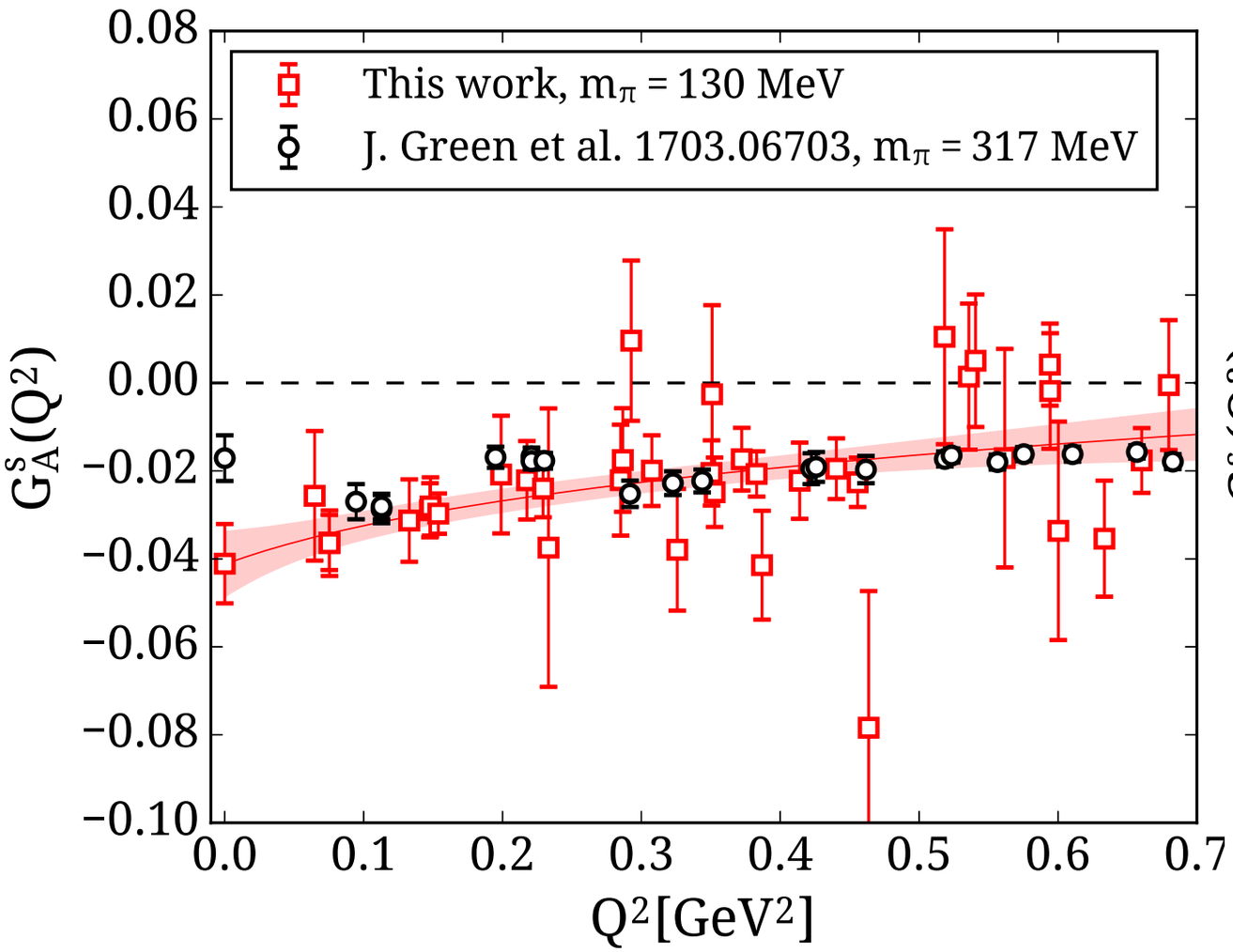


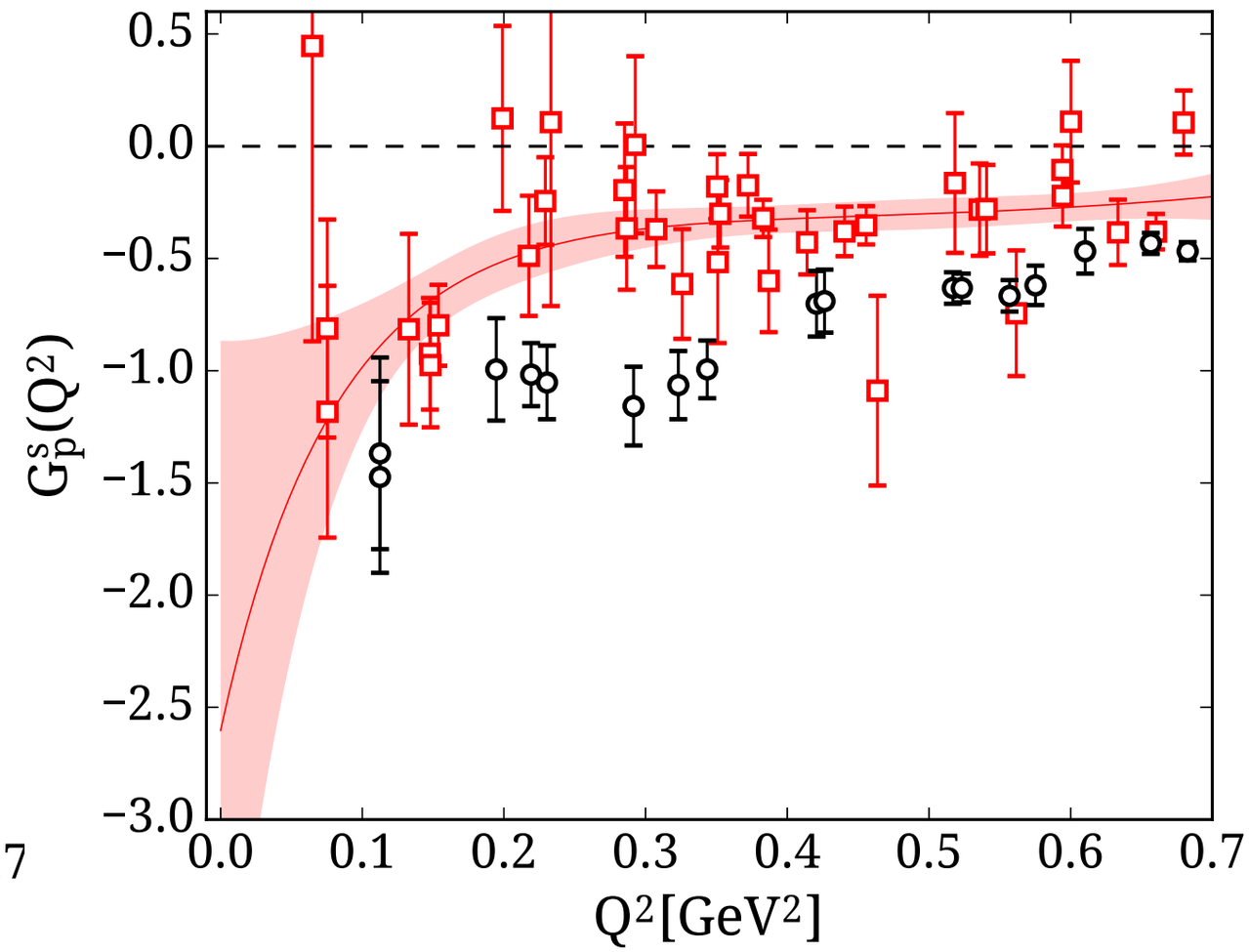


- Results for $G_A^s(Q^2)$ in good agreement except for small $Q^2$.
- Results for $G_p^s(Q^2)$, smaller in magnitude.

| | | |
|---|---|---|
| $N_{cnfs}$ | $\sim 2000$ | $\sim 1000$ |
| $N_{src}$ | 100 | 96 |

# Conclusions and future work

**Conclusions:**

- $G_A^{u-d}(Q^2)$ is compatible with the recent MiniBooNE experiment.
- The direct computation of the $G_p^{u-d}(Q^2)$ shows a weak $Q^2$ - dependence, whereas the result from pion pole dominance is compatible with the experimental results.
- The difference between the non-singlet and singlet axial renormalization factor is found to be small.
- **Disconnected contributions to axial and induced pseudoscalar form factors have been computed on a physical pion mass.**
- $G_A^{u+d}(Q^2)$ disconnected is negative as well as the $G_A^s(Q^2)$.
- $G_p^{u+d}(Q^2)$ disconnected is large negative with same magnitude as the connected.
- $G_p^s(Q^2)$ is found negative and non-zero.

# Conclusions and future work

## Conclusions:

- $G_A^{u-d}(Q^2)$ is compatible with the recent MiniBooNE experiment.
- The direct computation of the $G_p^{u-d}(Q^2)$ shows a weak $Q^2$ - dependence, whereas the result from pion pole dominance is compatible with the experimental results.
- The difference between the non-singlet and singlet axial renormalization factor is found to be small.
- **Disconnected contributions to axial and induced pseudoscalar form factors have been computed on a physical pion mass.**
- $G_A^{u+d}(Q^2)$ disconnected is negative as well as the $G_A^s(Q^2)$.
- $G_p^{u+d}(Q^2)$ disconnected is large negative with same magnitude as the connected.
- $G_p^s(Q^2)$ is found negative and non-zero.

## Future Work:

- Evaluation of disconnected contributions using a $N_f$ = 2+1+1 physical ensemble.
- Further study of noise reduction techniques.

# Backup Slides

$$R_\mu(\Gamma_\nu, \vec{q}; t_s, t_{\rm ins}) = \frac{G_\mu(\Gamma_\nu, \vec{q}; t_s, t_{\rm ins})}{C(\Gamma_0, \vec{0}; t_s)} \sqrt{\frac{C(\Gamma_0, \vec{q}; t_s - t_{\rm ins}) C(\Gamma_0, \vec{0}; t_{\rm ins}) C(\Gamma_0, \vec{0}; t_s)}{C(\Gamma_0, \vec{0}; t_s - t_{\rm ins}) C(\Gamma_0, \vec{q}; t_{\rm ins}) C(\Gamma_0, \vec{q}; t_s)}} \longrightarrow \Pi_\mu(\Gamma_\nu, \vec{q})$$

$$\begin{aligned} G_\mu(\vec{q}, t_s, t_{\rm ins}) &= A_{00}(\vec{q}) e^{-E_0(\vec{0})(t_s - t_{\rm ins}) - E_0(\vec{q}) t_{\rm ins}} + A_{01}(\vec{q}) e^{-E_0(\vec{0})(t_s - t_{\rm ins}) - E_1(\vec{q}) t_{\rm ins}} \\ &+ A_{10}(\vec{q}) e^{-E_1(\vec{0})(t_s - t_{\rm ins}) - E_0(\vec{q}) t_{\rm ins}} + A_{11}(\vec{q}) e^{-E_1(\vec{0})(t_s - t_{\rm ins}) - E_1(\vec{q}) t_{\rm ins}} \end{aligned}$$

$$C(\vec{q}, t_s) = c_0(\vec{q}) e^{-E_0(\vec{q}) t_s} + c_1(\vec{q}) e^{-E_1(\vec{q}) t_s}$$

$$\mathcal{M} = \frac{A_{00}(\vec{q})}{\sqrt{c_0(\vec{0}) c_0(\vec{q})}}.$$

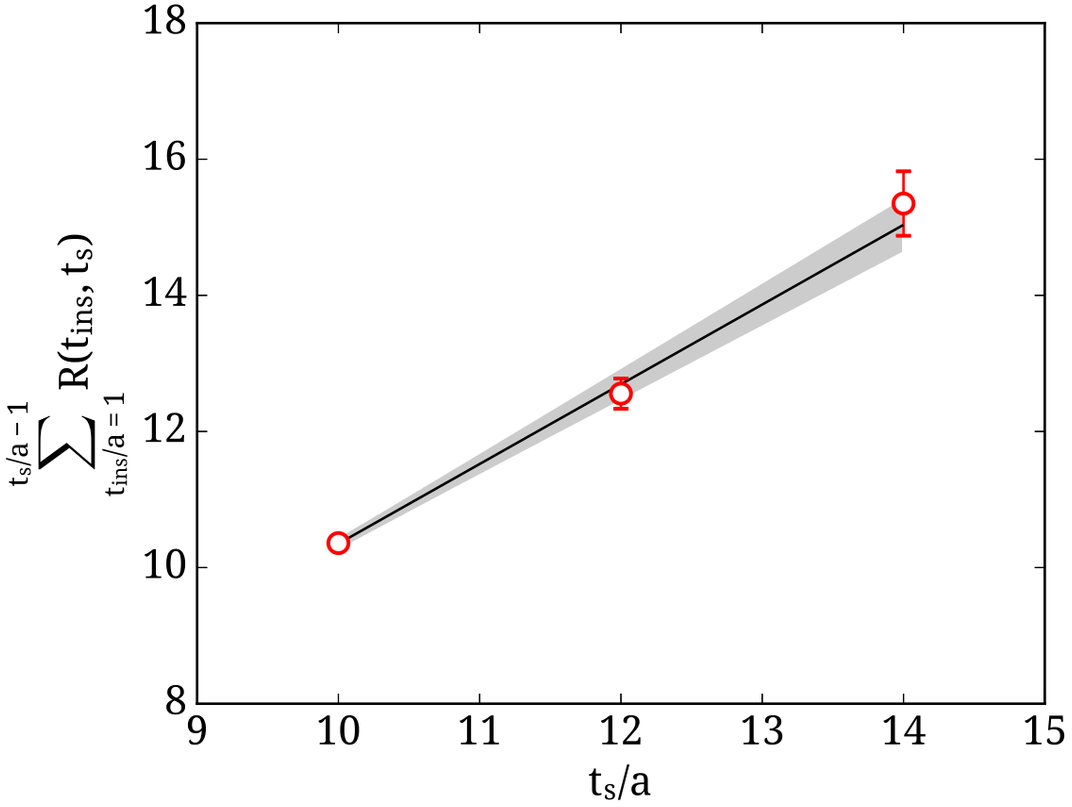


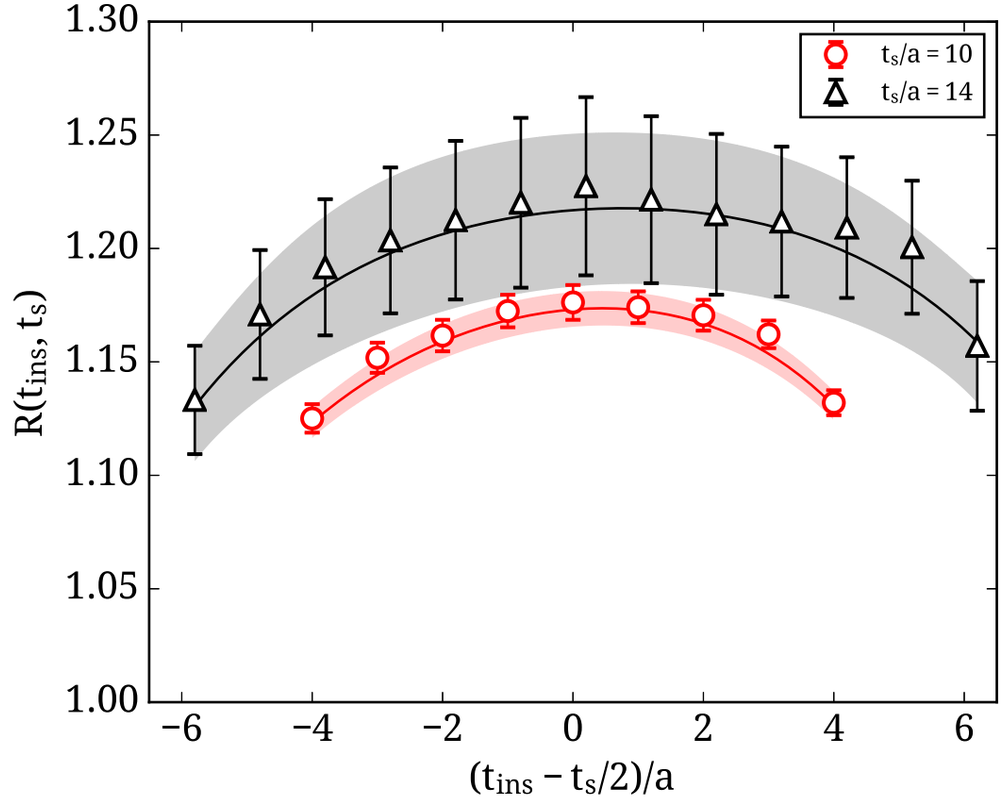

# Backup Slides

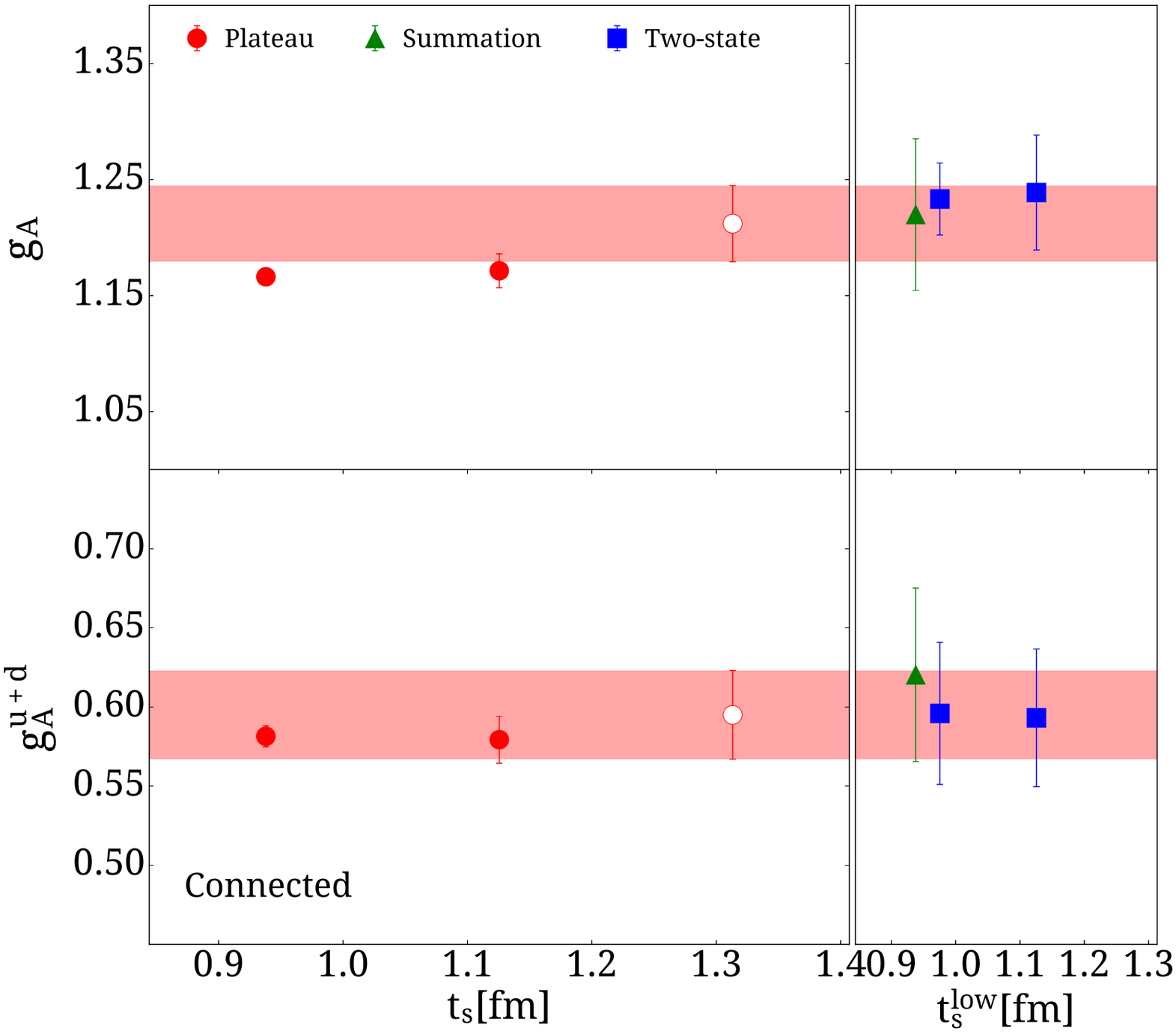

# Backup Slides

| | This work | Experiment |
|---|---|---|
| $g_A$ | 1.212(33)(22) | 1.2723(23) |
| $g_A^{u+d}$ (Conn.) | 0.595(28)(1) | - |
| $g_A^{u+d}$ (Disc.) | -0.150(20)(19) | - |
| $g_A^{u+d}$ | 0.445(34)(19) | 0.416(18) |
| $g_A^u$ | 0.827(30)(5) | 0.843(12) |
| $g_A^d$ | -0.380(15)(23) | -0.427(12) |
| $g_A^s$ | -0.0427(100)(93) | - |
| $g_A^c$ | -0.00338(188)(667) | - |

| Form factor | $m_A$ [GeV] | $\langle r_A^2 \rangle$ [fm$^2$] | $\chi^2$/d.o.f |
|---|---|---|---|
| $G_A^{u-d}$ | 1.322(42)(56) | 0.266(17)(7) | 0.35 |
| $G_A^{u+d}$ | 1.736(244)(374) | 0.155(43)(96) | 0.64 |
| $G_A^s$ | 0.823(175)(112) | 0.687(292)(155) | 0.30 |